MIMO Radar and Cellular Coexistence: A Power-Efficient Approach Enabled by Interference Exploitation

Fan Liu , *Student Member, IEEE*, Christos Masouros , *Senior Member, IEEE*, Ang Li , *Student Member, IEEE*, Tharmalingam Ratnarajah, *Senior Member, IEEE*, and Jianming Zhou

Abstract—We propose a novel approach to enable the coexistence between Multi-Input-Multi-Output (MIMO) radar and downlink multiuser multi-input single-output communication system. By exploiting the constructive multiuser interference (MUI), the proposed approach tradeoff useful MUI power for reducing the transmit power, to obtain a power efficient transmission. This paper focuses on two optimization problems: a) Transmit power minimization at the base station (BS), while guaranteeing the receive signal-to-interference-plus-noise ratio (SINR) level of downlink users and the interference-to-noise ratio level to radar; b) Minimization of the interference from BS to radar for a given requirement of downlink SINR and transmit power budget. To reduce the computational overhead of the proposed scheme in practice, an algorithm based on gradient projection is designed to solve the power minimization problem. In addition, we investigate the tradeoff between the performance of radar and communication, and analytically derive the key metrics for MIMO radar in the presence of the interference from the BS. Finally, a robust power minimization problem is formulated to ensure the effectiveness of the proposed method in the case of imperfect channel state information. Numerical results show that the proposed method achieves a significant power saving compared to conventional approaches, while obtaining a favorable performance-complexity tradeoff.

Index Terms—MU-MISO downlink, radar-communication coexistence, spectrum sharing, constructive interference.

I. INTRODUCTION

IN RESPONSE to the increasing demand for wireless communication devices and services, the Federal

Communications Commission (FCC) has adopted a broadband plan to release an additional 500 MHz spectrum that is currently occupied by military and governmental operations, such as air surveillance and weather radar systems [1]. Since then, spectrum sharing between radar and communication has been regarded as a promising solution. In [2], a radar information rate has been defined, such that the performance of radar and communication can be discussed using the same metric. Similar work has been done in [3], [4], in which radar and communication are unified under the framework of information theory, and the channel capacity between radar and target has been defined by applying the rate distortion theory. Nevertheless, these works focus on the theoretical performance analysis rather than practical waveform design. As an enabler, the approach of embedding communication information in the radar waveform has been proposed in [5]–[8], where important trade-offs have been revealed.

Recently, numerous approaches considering the spectral coexistence between MIMO radar and communications have been proposed [9]–[14]. In [9], the feasibility of combining MIMO radar and Orthogonal Frequency Division Multiplexing (OFDM) communications has been studied. More relevant to ths work, transmit beamforming has been viewed as a promising solution to eliminating the mutual interference between radar and communication. First pioneered by [10], the idea of null space projection (NSP) beamforming has been widely discussed [10]–[12], where the radar waveforms are projected onto the null space of the interference channel matrix from radar transmitter to communication receiver. However, it is clear that perfect CSI is unavailable in realistic scenarios. In view of this, the recent NSP work [12] introduces a practical interference channel estimation method. Optimization-based beamforming has been exploited to solve the problem in [13], where the SINR of radar has been optimized subject to power and capacity constraints of communication. Related work discusses the coexistence between MIMO-Matrix Completion (MIMO-MC) radar and point-to-point (P2P) MIMO communication system, where the radar beamforming matrix and communication covariance matrix are jointly optimized [14]. In contrast, the coexistence between MIMO radar and multi-user MIMO (MU-MIMO) communications has been discussed in [15]. In general, existing works on interference mitigation for coexistence mainly consider perfect or estimated CSI, and none of above works address the issue of robust beamforming with bounded or probabilistic CSI errors.

Motivated by the robust beamforming in the broader area of cognitive radio networks [16], [17], the work [18] investigated the robust MIMO beamforming for the coexistence of radar and downlink MU-MIMO communication, where the radar detection probability was maximized while guaranteeing the transmit power of BS and the receive SINR for each downlink user using Semidefinite Relaxation (SDR) techniques [19], [20]. In such optimizations, all the interference from other downlink users is regarded as harmful to the user of interest. Nevertheless, previous works proved that for a downlink MU-MIMO system using PSK modulations, the known interference can act constructively to benefit the symbol decision at downlink users [21]–[24]. Recent works [25], [26] showed that by rotating the destructive interference into constructive region using optimization techniques, the receive SINR target for each user was actually relaxed compared to the conventional SDR-based beamformer, thus a significant power saving was obtained. Given the significant advantage of the interference exploitation technique, it has been already applied to various research fields [27]–[33].

In this paper, we develop a novel precoding optimization approach for the spectrum sharing between MIMO radar and downlink MU-MISO communication based on the concept of constructive interference (CI). By allowing the BS to utilize the known interference as a green signal power, the feasible domain of the optimization problem is extended compared to the conventional SDR-based beamforming. We note that beamforming designs at both radar and cellular sides may facilitate a better performance. Nevertheless, such schemes are not practical at present, since the use of radar spectrum by communications requires that no changes are made to the government-run radar systems operation. We therefore consider beamforming methods only at the BS side, where two optimization-based transmit beamforming designs are proposed. The first one is to minimize the transmit power at the BS while guaranteeing the receive SINR at the users and the interference level from BS to radar, and the other is to minimize the total interference from BS to radar subject to the SINR constraint per user and transmit power budget. It is worth noting that both problems are convex and can be optimally solved by numerical tools. To efficiently apply the proposed schemes in practice, we design an efficient gradient projection algorithm for power minimization by analyzing the structure of the optimization. To investigate the effect of interference minimization beamforming on the performance of radar, we further derive the analytic form of detection probability and Cramér-Rao bound (CRB) for MIMO radar with the presence of the interference from the BS. By doing so, important trade-offs between the performance of radar and communication are given. Finally, we consider the uncertainty in the estimated channel information, and design a worst-case robust beamformer based on the principle of interference exploitation.

The remainder of this paper is organized as follows. Section II introduces the system model and briefly recalls the conventional SDR-based beamforming problems. Section III describes the concept of CI and formulates the proposed optimization problems using the CI technique. In Section IV, a thorough analysis for the power minimization optimization is present and an efficient algorithm is derived. Section V
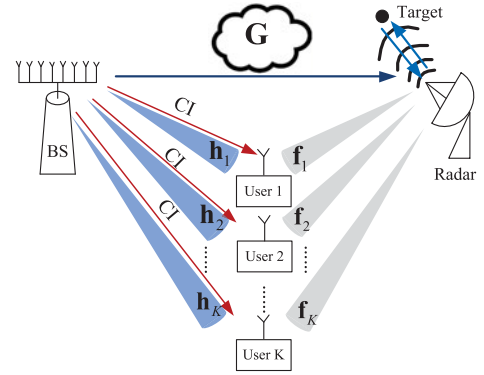

Fig. 1. Spectrum sharing scenario.

derives the detection probability and the Cramér-Rao bound of MIMO radar for the proposed scenario. A worst-case approach for imperfect CSI is given for robust power minimization in Section VI, with norm-bounded CSI errors. Numerical results are provided and discussed in Section VII. Finally, Section VIII concludes the paper.

Notations: Matrices are denoted by bold uppercase letters (i.e., $\mathbf{H}$), bold lowercase letters are used for vectors (i.e., $\boldsymbol{\beta}$), subscripts indicate the rows of a matrix unless otherwise specified (i.e., $\mathbf{h}_i$ is the i-th column of $\mathbf{H}$), scalars are denoted by normal font (i.e., R_m), $\mathrm{tr}(\cdot)$ stands for the trace of the argument, $(\cdot)^T$, $(\cdot)^*$ and $(\cdot)^H$ stand for transpose, complex conjugate and Hermitian transpose respectively, $\mathrm{Re}(\cdot)$ and $\mathrm{Im}(\cdot)$ denote the real and imaginary part of the argument.

II. SYSTEM MODEL AND SDR-BASED BEAMFORMING

Consider a spectrum sharing scenario where a K-user MU-MISO downlink system operates at the same frequency band with a MIMO radar. As can be seen in Fig. 1, the N-antenna BS is transmitting signals to K single-antenna users while the MIMO radar with M_t transmit antennas and M_r receive antennas is detecting a point-like target in the far-field. Inevitably, these two systems will cause interference to each other. The received signal at the i-th user is given as

$$y_i^C[l] = \mathbf{h}_i^T \sum_{k=1}^{K} \mathbf{t}_k d_k[l] + \sqrt{P_R} \mathbf{f}_i^T \mathbf{s}_l + n_i[l], i = 1, 2, \ldots, K,$$

(1)

where $\mathbf{h}_i \in \mathbb{C}^{N \times 1}$ denotes the communication channel vector, $\mathbf{f}_i \in \mathbb{C}^{M_t \times 1}$ denotes the interference channel vector from radar to the user, $\mathbf{t}_i \in \mathbb{C}^{N \times 1}$ denotes the precoding vector, $d_i[l]$ and $n_i[l] \sim \mathcal{CN}(0, \sigma_C^2)$ stands for the communication symbol and the received noise for the i-th user. The second term at the right hand of (1) denotes the interference from radar to the user, where $\mathbf{S} = [\mathbf{s}_1, \mathbf{s}_2, \ldots, \mathbf{s}_{L_R}] \in \mathbb{C}^{M_t \times L_R}$ are the radar transmit waveforms, $l = 1, 2, \ldots, L$ is the communication symbol index, and P_R is the power of radar signal.

With the presence of a point-like target located at direction θ, the echo wave that received by radar at the l-th time slot is

$$\mathbf{y}_l^R = \alpha \sqrt{P_R} \mathbf{A}(\theta) \mathbf{s}_l + \mathbf{G}^T \sum_{k=1}^{K} \mathbf{t}_k d_k[l] + \mathbf{z}_l, \qquad (2)$$

where $\mathbf{G} = [\mathbf{g}_1, \mathbf{g}_2, \ldots, \mathbf{g}_{M_r}] \in \mathbb{C}^{N \times M_r}$ is the interference channel matrix between the BS transmitter and the radar receiver, $\alpha \in \mathbb{C}$ is the complex path loss of the path between radar and target, $\mathbf{z}_l = [z_1[l], z_2[l], \ldots, z_{M_r}[l]]^T \in \mathbb{C}^{M_r \times 1}$ is the received noise at the l-th snapshot with $z_m[l] \sim \mathcal{CN}(0, \sigma_R^2), \forall m$, $\mathbf{A}(\theta) = \mathbf{a}_R(\theta)\mathbf{a}_T^T(\theta)$, in which $\mathbf{a}_T(\theta) \in \mathbb{C}^{M_t \times 1}$ and $\mathbf{a}_R(\theta) \in \mathbb{C}^{M_r \times 1}$ are transmit and receive steering vectors of the radar antenna array. The model in (2) is assumed to be obtained in a single range-Doppler bin of the radar detector and thus omits the range and Doppler parameters. In this paper, we apply the basic assumptions in [34] on the radar model, which is

$$M_r = M_t = M, \quad \mathbf{a}_R(\theta) = \mathbf{a}_T(\theta) = \mathbf{a}(\theta),$$

$$\mathbf{A}_{im}(\theta) = \mathbf{a}_i(\theta)\mathbf{a}_m(\theta) = e^{-j\omega\tau_{im}(\theta)} \quad (3)$$

$$= e^{\left(-j\frac{2\pi}{\lambda}[\sin(\theta);\cos(\theta)]^T(\mathbf{x}_i + \mathbf{x}_m)\right)},$$

where ω and λ denote the frequency and the wavelength of the carrier, $\mathbf{A}_{im}(\theta)$ is the i-th element at the m-th column of the matrix $\mathbf{A}$, which is the total phase delay of the signal that transmitted by the i-th element and received by the m-th element of the antenna array, and $\mathbf{x}_i = [x_i^1; x_i^2]$ is the location of the i-th element of the antenna array.

Without loss of generality, we rely on the following assumptions:

1) For notational simplicity, the communication symbol is drawn from a normalized PSK constellation, while we note that the proposed concept of interference exploitation has been shown to offer benefits for other modulation formats, such as Quadrature Amplitude Modulation (QAM) [29], [35]. The PSK symbol can be denoted as $d_k[l] = e^{j\phi_k[l]}$.

2) Following the typical assumptions in the radar-communication literature [10], [11], [14], we assume that $\mathbf{H} = [\mathbf{h}_1, \mathbf{h}_2, \ldots, \mathbf{h}_K]$, $\mathbf{F} = [\mathbf{f}_1, \mathbf{f}_2, \ldots, \mathbf{f}_K]$ and $\mathbf{G} = [\mathbf{g}_1, \mathbf{g}_2, \ldots, \mathbf{g}_K]$ are flat Rayleigh fading and statistically independent with each other.

3) According to the standard assumption in MIMO radar literature [34], [36], $\mathbf{S}$ is set to be orthogonal, i.e., $\mathbb{E}[\mathbf{s}_l\mathbf{s}_l^H] = \frac{1}{L_R}\sum_{l=1}^{L_R}\mathbf{s}_l\mathbf{s}_l^H = \mathbf{I}$, where $\mathbb{E}$ denotes the ensemble average.

4) In the radar signal model, it is assumed that the communication interference is the only interference received by radar. Following the closely related literature, the interference caused by clutter and false targets is not considered [11].

5) The duration of the radar sub-pulse is assumed to be the same as the communication symbol duration. According to [14], this is applicable to the practical scenario, since the duration of the sub-pulse of an S-band radar falls into the typical range of the symbol interval in LTE systems. It should be highlighted that in order to preserve the orthogonality of $\mathbf{S}$, radar may utilize codeword that is longer than a typical communication frame. Without loss of generality, we assume $L_R = L$ for the ease of our derivation.

6) The channels are assumed to be known to the BS. For the communication channel $\mathbf{H}$, the conventional estimation techniques can be used to acquire the CSI. For the interference channels $\mathbf{G}$ and $\mathbf{F}$, we adopt the approach proposed in [37], i.e., to estimate CSI by the coordination of a control center with abundant computing resources, which also serves as the radar fusion center.

For convenience, we omit the time index l in the rest of the paper unless otherwise specified. Under the above assumptions, the receive SINR at the i-th user is given by

$$\gamma_i = \frac{\left|\mathbf{h}_i^T\mathbf{t}_i\right|^2}{\sum_{k=1, k\neq i}^{K}\left|\mathbf{h}_i^T\mathbf{t}_k\right|^2 + P_R\|\mathbf{f}_i\|^2 + \sigma_C^2}, \forall i. \quad (4)$$

And the average transmit power of the BS is

$$P_C = \sum_{k=1}^{K}\|\mathbf{t}_k\|^2. \quad (5)$$

The interference from the BS on the m-th antenna of radar is given by

$$u_m = \mathbf{g}_m^T\sum_{k=1}^{K}\mathbf{t}_k d_k. \quad (6)$$

We define the average INR at the m-th receive antenna of radar as

$$r_m = \frac{\mathbb{E}\left(|u_m|^2\right)}{\sigma_R^2} = \frac{\text{tr}\left(\mathbf{g}_m^*\mathbf{g}_m^T\sum_{k=1}^{K}\mathbf{t}_k\mathbf{t}_k^H\right)}{\sigma_R^2}. \quad (7)$$

From a conventional perspective, all interference should be treated as harmful when optimizing the performance of the two systems. The power minimization problem of the BS subject to INR and SINR thresholds is formulated as

$$\mathcal{P}_0 : \min_{\mathbf{t}_k} \quad P_C$$

$$s.t. \quad \gamma_i \geq \Gamma_i, \forall i,$$

$$r_m \leq R_m, \forall m, \quad (8)$$

where Γ_i is the required SINR of the i-th communication user, R_m is the maximum tolerable INR level of the m-th receive element of radar. Note that the MIMO radar is typically equipped with independent RF chains at different antennas, whose dynamic-range (DR) performance determines the minimum and maximum distances that the radar can observe. In order to guarantee the DR performance of individual RF chains, we impose a per-antenna interference constraint in the optimization problem, such that the interference received by each RF chain is lower than the given threshold.

Similarly, we can formulate the optimization problem that maximizes the detection probability of radar while guaranteeing the BS power and the required SINR level at each user. This is given as

$$\mathcal{P}_1 : \max_{\mathbf{t}_k} \quad P_D$$

$$s.t. \quad \gamma_i \geq \Gamma_i, \forall i,$$
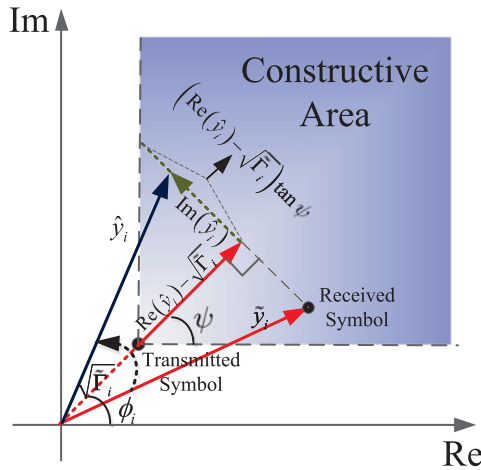
$$P_C \leq P, \quad (9)$$

Fig. 2.   The principle of constructive interference.

where P_D is the detection probability, and P is the budget of the BS transmit power. The objective function of the above problem is non-convex. Fortunately, according to [18], $\mathcal{P}_1$ can be relaxed as a lower-bound maximization problem, which can be equivalently given as

$$\mathcal{P}_2 : \min_{\mathbf{t}_k} \ \sum_{m=1}^{M} r_m \sigma_R^2$$

$$s.t. \ \gamma_i \geq \Gamma_i, \forall i,$$

$$P_C \leq P. \qquad (10)$$

This is to minimize the interference from BS to radar. Readers can refer to [18] for a detailed derivation. Problem $\mathcal{P}_0$ and $\mathcal{P}_2$ can be readily transformed into Semidefinite Program (SDP) [38] with Semidefinite Relaxation techniques, and thus can be solved by numerical tools. We refer readers to [18]–[20] for more details on this topic. As shown in Fig. 1 by red arrows, it is worth noting the above problems ignore the fact that for each user, interference from other users can contribute to the received signal power constructively. In this paper, we aim to show that the solution of these problems is suboptimal from an instantaneous point of view and design a symbol-based beamforming method in accordance to the concept of constructive interference.

III. BEAMFORMING WITH CONSTRUCTIVE INTERFERENCE

As per the model of [26], the instantaneous interference can be divided into two categories, constructive interference and destructive interference. Generally, the constructive interference is defined as the interference that moves the received symbol away from the decision thresholds. The purpose of the CI-based beamforming is to rotate the known interference from other users such that the resultant received symbol falls into the constructive region. This is shown in Fig. 2, where we denote the constructive area of the QPSK symbol by the blue shade. It has been proven in [26] that the optimization will become more relaxed than conventional interference cancellation optimizations due to the expansion of the optimization region. Hence, the performance of the beamformer is improved. Here we consider the instantaneous transmit power, which is given as

$$P_T = \left\| \sum_{k=1}^{K} \mathbf{t}_k e^{j(\phi_k - \phi_1)} \right\|^2 , \qquad (11)$$

where $d_1 = e^{j\phi_1}$ is used as the phase reference. For notational simplicity we omit the time index l. Based on [26], we consider the instantaneous SINR constraints. Note that if all the multi-user interference (MUI) contributes to the received symbol, the instantaneous SINR constraint of the i-th user is given by

$$\tilde{\gamma}_i = \frac{\left| \mathbf{h}_i^T \sum_{k=1}^{K} e^{j\phi_k} \right|^2}{P_R \left| \mathbf{f}^T \mathbf{s} \right|^2 + \sigma_C^2} \geq \Gamma_i, \qquad (12)$$

where $\mathbf{s}$ is the radar signal vector. It follows that

$$\left| \mathbf{h}_i^T \sum_{k=1}^{K} e^{j\phi_k} \right| - \sqrt{\tilde{\Gamma}_i} \geq 0, \qquad (13)$$

where $\tilde{\Gamma}_i = \Gamma_i (P_R |\mathbf{f}^T \mathbf{s}|^2 + \sigma_C^2)$.

Let us denote the noise-free received signal as $\tilde{y}_i = \mathbf{h}_i^T \sum_{k=1}^{K} e^{j\phi_k}$. To formulate the constructive constraint, we consider a simple phase rotation of $\tilde{y}_i$, which rotates the received symbol into the reference system of the desired symbol $d_i = e^{j\phi_i}$. This is

$$\hat{y}_i = \tilde{y}_i e^{-j\phi_i} = \mathbf{h}_i^T \sum_{k=1}^{K} e^{j(\phi_k - \phi_i)}. \qquad (14)$$

The geometric relations of the above variables are shown in Fig. 2, where a QPSK symbol is taken as example. It is easy to see that for the received symbol that falls into the constructive area, we have

$$|\text{Im}(\hat{y}_i)| \leq \left(\text{Re}(\hat{y}_i) - \tilde{\Gamma}_i \right) \tan \psi, \qquad (15)$$

where $\psi = \frac{\pi}{M_p}$, and M_p is the PSK modulation order. By substituting (14) into (15), the CI constraints are given as

$$\left| \text{Im} \left(\mathbf{h}_i^T \sum_{k=1}^{K} \mathbf{t}_k e^{j(\phi_k - \phi_i)} \right) \right|$$

$$\leq \left(\text{Re} \left(\mathbf{h}_i^T \sum_{k=1}^{K} \mathbf{t}_k e^{j(\phi_k - \phi_i)} \right) - \sqrt{\tilde{\Gamma}_i} \right) \tan \psi, \forall i, \qquad (16)$$

Readers are referred to [26] for a detailed derivation of the CI constraints and classification. Finally, similar to the SDR case, the instantaneous interference constraints can be obtained as

$$\left| \mathbf{g}_m^T \sum_{k=1}^{K} \mathbf{t}_k e^{j\phi_k} \right|^2 \leq R_m \sigma_R^2, \forall m. \qquad (17)$$

Based on above, we reformulate the power minimization problem $\mathcal{P}_0$ as the CI based problem $\mathcal{P}_3$, which is

$$\mathcal{P}_3 : \min_{\mathbf{t}_k} \ P_T$$

$$s.t. \ \text{Constraints (16) and (17)}, \qquad (18)$$

where P_T is given by (11).

It should be highlighted that, while here we focus on PSK constellations, the optimizations $\mathcal{P}_3$ onwards can be readily adapted to QAM modulations [29], [35]. Note that $\mathcal{P}_3$ is convex in contrast to the non-convex counterparts $\mathcal{P}_0$ and $\mathcal{P}_2$, for which only sub-optimal solutions can be obtained via the complicated SDR method. On the contrary, problem $\mathcal{P}_3$ is a second-order cone program (SOCP) and can be solved optimally by simpler numerical solvers.

In both $\mathcal{P}_0$ and $\mathcal{P}_3$, by letting $R_m = 0$, it follows $\mathbf{g}_m^T \sum_{k=1}^{K} \mathbf{t}_k d_k = 0$, which requires the transmitting signal to fall into the null space of the interference matrix $\mathbf{G}$ and causes zero interference to radar. This yields the solution with which the radar can achieve the best performance. However, the strict equality will result in a large transmit power at BS. On the other hand, if we let $R_m \to \infty$, the INR constraints will be ineffective, which is equivalent to the typical downlink power minimization in the absence of radar. This trade-off between radar and communication performance will be further evaluated by numerical simulations.

It can be further noted that, by incorporating the desired symbol into the channel vector, $\mathcal{P}_3$ can be readily transformed into a simpler virtual multicast model. To illustrate this, we denote $\mathbf{w} \triangleq \sum_{k=1}^{K} \mathbf{t}_k e^{j(\phi_k - \phi_1)}$, $\tilde{\mathbf{h}}_i \triangleq \mathbf{h}_i e^{j(\phi_1 - \phi_i)}$, $\tilde{\mathbf{g}}_m \triangleq \mathbf{g}_m e^{j\phi_1}$, the power minimization problem $\mathcal{P}_3$ can be equivalently written as

$$\mathcal{P}_4 : \min_{\mathbf{w}} \|\mathbf{w}\|^2$$

$$s.t. \left| \text{Im}\left(\tilde{\mathbf{h}}_i^T \mathbf{w} \right) \right| \leq \left(\text{Re}\left(\tilde{\mathbf{h}}_i^T \mathbf{w} \right) - \sqrt{\tilde{\Gamma}_i} \right) \tan \psi, \forall i,$$

$$\left| \tilde{\mathbf{g}}_m^T \mathbf{w} \right| \leq \sqrt{R_m \sigma_R^2}, \forall m, \tag{19}$$

Similarly, the CI-based interference minimization problem is given by

$$\mathcal{P}_5 : \min_{\mathbf{w}} \sum_{m=1}^{M} \left| \tilde{\mathbf{g}}_m^T \mathbf{w} \right|^2$$

$$s.t. \left| \text{Im}\left(\tilde{\mathbf{h}}_i^T \mathbf{w} \right) \right| \leq \left(\text{Re}\left(\tilde{\mathbf{h}}_i^T \mathbf{w} \right) - \sqrt{\tilde{\Gamma}_i} \right) \tan \psi, \forall i,$$

$$\|\mathbf{w}\| \leq \sqrt{P}. \tag{20}$$

After obtaining the optimal solution $\mathbf{w}$, the beamforming vectors can be obtained as

$$\mathbf{t}_k = \frac{\mathbf{w} e^{j(\phi_1 - \phi_k)}}{K}, \forall k. \tag{21}$$

Note that both $\mathcal{P}_4$ and $\mathcal{P}_5$ are convex and can be easily solved by numerical tools. To make the proposed method more realizable in practical scenarios, we will take $\mathcal{P}_4$ as an example to derive an efficient algorithm to solve it, and a similar algorithm can be also applied to $\mathcal{P}_5$.

IV. EFFICIENT ALGORITHM FOR POWER MINIMIZATION BEAMFORMING

A. Real Representation of the Problem

For the ease of our further analysis, we first derive the real representation of the problem. Let us rewrite the related channel vectors and the beamforming vector as follows

$$\tilde{\mathbf{h}}_i = \tilde{\mathbf{h}}_{Ri} + j\tilde{\mathbf{h}}_{Ii}, \tilde{\mathbf{g}}_m = \tilde{\mathbf{g}}_{Rm} + j\tilde{\mathbf{g}}_{Im}, \mathbf{w} = \mathbf{w}_R + j\mathbf{w}_I, \tag{22}$$

where

$$\tilde{\mathbf{h}}_{Ri} = \text{Re}\left(\tilde{\mathbf{h}}_i \right), \tilde{\mathbf{h}}_{Ii} = \text{Im}\left(\tilde{\mathbf{h}}_i \right), \tilde{\mathbf{g}}_{Rm} = \text{Re}\left(\tilde{\mathbf{g}}_m \right),$$

$$\tilde{\mathbf{g}}_{Im} = \text{Im}\left(\tilde{\mathbf{g}}_m \right), \mathbf{w}_R = \text{Re}\left(\mathbf{w} \right), \mathbf{w}_I = \text{Im}\left(\mathbf{w} \right). \tag{23}$$

Then we define the following real-valued vectors and matrices

$$\bar{\mathbf{h}}_i = \left[\tilde{\mathbf{h}}_{Ri}; \tilde{\mathbf{h}}_{Ii} \right], \mathbf{w}_1 = \left[\mathbf{w}_I; \mathbf{w}_R \right], \mathbf{w}_2 = \left[\mathbf{w}_R; -\mathbf{w}_I \right],$$

$$\boldsymbol{\beta}_m = \begin{bmatrix} \tilde{\mathbf{g}}_{Rm} & \tilde{\mathbf{g}}_{Im} \\ \tilde{\mathbf{g}}_{Im} & -\tilde{\mathbf{g}}_{Rm} \end{bmatrix}, \boldsymbol{\Pi} = \begin{bmatrix} \mathbf{0}_K & -\mathbf{I}_K \\ \mathbf{I}_K & \mathbf{0}_K \end{bmatrix}, \tag{24}$$

where $\mathbf{I}_K$ and $\mathbf{0}_K$ denote the $K \times K$ identity matrix and all-zero matrix respectively. Thus we obtain

$$\text{Re}\left(\tilde{\mathbf{h}}_i^T \mathbf{w} \right) = \bar{\mathbf{h}}_i^T \mathbf{w}_2, \text{Im}\left(\tilde{\mathbf{h}}_i^T \mathbf{w} \right) = \bar{\mathbf{h}}_i^T \boldsymbol{\Pi} \mathbf{w}_2 \triangleq \mathbf{b}_i^T \mathbf{w}_2,$$

$$\left| \tilde{\mathbf{g}}_m^T \mathbf{w} \right|^2 = \left\| \begin{bmatrix} \tilde{\mathbf{g}}_{Rm}^T & \tilde{\mathbf{g}}_{Im}^T \\ \tilde{\mathbf{g}}_{Im}^T & -\tilde{\mathbf{g}}_{Rm}^T \end{bmatrix} \begin{bmatrix} \mathbf{w}_R \\ -\mathbf{w}_I \end{bmatrix} \right\|^2 = \left\| \boldsymbol{\beta}_m^T \mathbf{w}_2 \right\|^2. \tag{25}$$

Finally, the real version of the problem is given as

$$\mathcal{P}_6 : \min_{\mathbf{w}_2} \|\mathbf{w}_2\|^2$$

$$s.t. \mathbf{b}_i^T \mathbf{w}_2 - \bar{\mathbf{h}}_i^T \mathbf{w}_2 \tan \psi + \sqrt{\tilde{\Gamma}_i} \tan \psi \leq 0, \forall i,$$

$$- \mathbf{b}_i^T \mathbf{w}_2 - \bar{\mathbf{h}}_i^T \mathbf{w}_2 \tan \psi + \sqrt{\tilde{\Gamma}_i} \tan \psi \leq 0, \forall i,$$

$$\left\| \boldsymbol{\beta}_m^T \mathbf{w}_2 \right\|^2 \leq R_m \sigma_R^2, \forall m. \tag{26}$$

B. The Dual Problem

In order to reveal the structure of the solution, we formulate the dual problem of $\mathcal{P}_6$. Let us define the dual variable that associate with the three constraints in (26) as $\mathbf{u}, \mathbf{v}, \mathbf{c}$ respectively, where $u_i \geq 0, v_i \geq 0, c_m \geq 0, \forall i, \forall m$ are the elements of the three dual vectors. The corresponding Lagrangian is given as (27) shown at the bottom of the next page. By the following definitions

$$\bar{\mathbf{h}} = \left[\bar{\mathbf{h}}_1, \bar{\mathbf{h}}_2, \dots, \bar{\mathbf{h}}_K \right], \mathbf{b} = \left[\mathbf{b}_1, \mathbf{b}_2, \dots, \mathbf{b}_K \right], \mathbf{1} = \left[\mathbf{I}_K; \mathbf{I}_K \right],$$

$$\boldsymbol{\lambda} = \left[\mathbf{u}; \mathbf{v} \right], \boldsymbol{\beta} = \left[\boldsymbol{\beta}_1, \boldsymbol{\beta}_2, \dots, \boldsymbol{\beta}_M \right], \mathbf{R} = \left[R_1, R_2, \dots, R_M \right],$$

$$\mathbf{c} = \left[c_1; c_2; \dots; c_M \right], \tilde{\mathbf{c}} = \left[c_1; c_1; c_2; c_2; \dots; c_M; c_M \right],$$

$$\tilde{\boldsymbol{\Gamma}} = \left[\tilde{\Gamma}_1; \tilde{\Gamma}_2; \dots; \tilde{\Gamma}_K \right], \mathbf{A} = \left[\bar{\mathbf{h}} \tan \psi - \mathbf{b}, \bar{\mathbf{h}} \tan \psi + \mathbf{b} \right], \tag{28}$$

the Lagrangian can be further simplified as

$$\mathcal{L}\left(\mathbf{w}_2, \mathbf{u}, \mathbf{v}, \mathbf{c}\right) = \mathbf{w}_2^T \left(\mathbf{I} + \boldsymbol{\beta} \operatorname{diag}\left(\tilde{\mathbf{c}}\right) \boldsymbol{\beta}^T\right) \mathbf{w}_2 + \boldsymbol{\lambda}^T \mathbf{A}^T \mathbf{w}_2$$

$$+ \tan \psi \sqrt{\tilde{\boldsymbol{\Gamma}}^T} \mathbf{1}^T \boldsymbol{\lambda} - \sigma_R^2 \mathbf{R}^T \mathbf{c}, \qquad (29)$$

where $\operatorname{diag}(\mathbf{x})$ denotes the diagonal matrix whose diagonal elements are given by $\mathbf{x}$. Let $\frac{\partial \mathcal{L}}{\partial \mathbf{w}_2} = 0$, the optimal solution of $\mathbf{w}_2$ is given by

$$\mathbf{w}_2^* = -\frac{\left(\mathbf{I} + \boldsymbol{\beta} \operatorname{diag}\left(\tilde{\mathbf{c}}\right) \boldsymbol{\beta}^T\right)^{-1} \mathbf{A} \boldsymbol{\lambda}}{2}, \qquad (30)$$

which implies $\boldsymbol{\lambda} \neq \mathbf{0}$, for the reason that $\boldsymbol{\lambda} = \mathbf{0}$ yields the trivial solution of $\mathbf{w}_2^* = \mathbf{0}$. Substituting the optimal $\mathbf{w}_2^*$ into the Lagrangian leads to

$$\mathcal{L}\left(\mathbf{u}, \mathbf{v}, \mathbf{c}\right) = -\frac{1}{4} \boldsymbol{\lambda}^T \mathbf{A}^T \left(\mathbf{I} + \boldsymbol{\beta} \operatorname{diag}\left(\tilde{\mathbf{c}}\right) \boldsymbol{\beta}^T\right)^{-1} \mathbf{A} \boldsymbol{\lambda}$$

$$+ \tan \psi \sqrt{\tilde{\boldsymbol{\Gamma}}^T} \mathbf{1}^T \boldsymbol{\lambda} - \sigma_R^2 \mathbf{R}^T \mathbf{c}. \qquad (31)$$

Therefore, the dual problem is given as

$$\mathcal{P}_7: \quad \max_{\boldsymbol{\lambda}, \mathbf{c}} \quad -\frac{1}{4} \boldsymbol{\lambda}^T \mathbf{A}^T \left(\mathbf{I} + \boldsymbol{\beta} \operatorname{diag}\left(\tilde{\mathbf{c}}\right) \boldsymbol{\beta}^T\right)^{-1} \mathbf{A} \boldsymbol{\lambda}$$

$$+ \tan \psi \sqrt{\tilde{\boldsymbol{\Gamma}}^T} \mathbf{1}^T \boldsymbol{\lambda} - \sigma_R^2 \mathbf{R}^T \mathbf{c}$$

$$s.t. \quad \boldsymbol{\lambda} \geq \mathbf{0}, \mathbf{c} \geq \mathbf{0}. \qquad (32)$$

Note that when removing the INR constraints, the dual problem is the same as the original CI-based power minimization problem in [26].

C. Efficient Gradient Projection Method

Let us first rewrite the dual problem as the following standard convex form

$$\mathcal{P}_8: \quad \min_{\boldsymbol{\lambda}, \mathbf{c}} \quad f\left(\boldsymbol{\lambda}, \mathbf{c}\right) = \frac{1}{4} \boldsymbol{\lambda}^T \mathbf{A}^T \left(\mathbf{I} + \boldsymbol{\beta} \operatorname{diag}\left(\tilde{\mathbf{c}}\right) \boldsymbol{\beta}^T\right)^{-1} \mathbf{A} \boldsymbol{\lambda}$$

$$- \tan \psi \sqrt{\tilde{\boldsymbol{\Gamma}}^T} \mathbf{1}^T \boldsymbol{\lambda} + \sigma_R^2 \mathbf{R}^T \mathbf{c}$$

$$s.t. \quad \boldsymbol{\lambda} \geq \mathbf{0}, \mathbf{c} \geq \mathbf{0}. \qquad (33)$$

It is easy to observe that the primal problem $\mathcal{P}_8$ is a convex Quadratically Constrained Quadratic Program (QCQP). Note that if $\mathbf{c} = \mathbf{0}$, $\mathcal{P}_8$ becomes a standard non-negative least square (NNLS) problem, whose closed-form is known to be difficult

---

Algorithm 1: Gradient Projection Method for Solving (26)

Input: $\mathbf{H}, \mathbf{G}, \mathbf{F}, \boldsymbol{\Gamma}, \mathbf{R}, \sigma_c, \sigma_R$.
Output: Optimal solution $\mathbf{w}_2^*$ for problem $\mathcal{P}_5$.
1: Initialize randomly $\boldsymbol{\lambda}^{(0)} \geq 0, \mathbf{c}^{(0)} \geq 0$.
2: In the ith iteration, update $\boldsymbol{\lambda}$ and $\mathbf{c}$ by:

$$\left[\boldsymbol{\lambda}^{(i)}, \mathbf{c}^{(i)}\right] = \max \left(\left[\boldsymbol{\lambda}^{(i)}, \mathbf{c}^{(i)}\right] - a_i \nabla f\left(\boldsymbol{\lambda}^{(i-1)}, \mathbf{c}^{(i-1)}\right), \mathbf{0}\right),$$

where the step size a_i is calculated by the backtracking linesearch method.
3: Go back to 2 until convergence.
4: Calculate $\mathbf{w}_2^*$ by

$$\mathbf{w}_2^* = -\frac{\left(\mathbf{I} + \boldsymbol{\beta} \operatorname{diag}\left(\tilde{\mathbf{c}}^{(i)}\right) \boldsymbol{\beta}^T\right)^{-1} \mathbf{A} \boldsymbol{\lambda}^{(i)}}{2}.$$

5: **end**

---

to obtain [39]. The newly added variable will further complicate the problem. Nevertheless, thanks to the simple constraints with only bounds on the variables, it is convenient to apply a gradient projection algorithm to solve the problem [40]. We then derive the gradient of the dual function as follows. By letting $\mathbf{M} = (\mathbf{I} + \boldsymbol{\beta} \operatorname{diag}(\tilde{\mathbf{c}}) \boldsymbol{\beta}^T)^{-1}$, the derivative is given as

$$\frac{\partial f}{\partial \boldsymbol{\lambda}} = \frac{1}{2} \boldsymbol{\lambda}^T \mathbf{A}^T \mathbf{M} \mathbf{A} - \tan \psi \sqrt{\tilde{\boldsymbol{\Gamma}}^T} \mathbf{1}^T,$$

$$\frac{\partial f}{\partial c_m} = -\frac{1}{4} \left| \boldsymbol{\lambda}^T \mathbf{A}^T \mathbf{M} \boldsymbol{\beta}_m \right|^2 + \sigma_R^2 R_m, \forall m. \qquad (34)$$

Thus the gradient is give by

$$\nabla f\left(\boldsymbol{\lambda}, \mathbf{c}\right) = \left[\frac{\partial f}{\partial \boldsymbol{\lambda}}, \frac{\partial f}{\partial \mathbf{c}}\right]^T = \begin{bmatrix} \frac{1}{2} \mathbf{A}^T \mathbf{M} \mathbf{A} \boldsymbol{\lambda} - \tan \psi \mathbf{1} \sqrt{\tilde{\boldsymbol{\Gamma}}}; \\ -\frac{1}{4} \left| \boldsymbol{\lambda}^T \mathbf{A}^T \mathbf{M} \boldsymbol{\beta}_1 \right|^2 + \sigma_R^2 R_1; \\ \dots \\ -\frac{1}{4} \left| \boldsymbol{\lambda}^T \mathbf{A}^T \mathbf{M} \boldsymbol{\beta}_M \right|^2 + \sigma_R^2 R_M \end{bmatrix}. \qquad (35)$$

Based on above derivations, the following Algorithm 1 is proposed to solve problem $\mathcal{P}_8$, where we use an iterative gradient projection method, and the step size can be decided by the Armijo rule or other backtracking linesearch methods [40]. After obtaining the optimal $\mathbf{w}_2$, the beamforming vectors can be calculated by (21).

$$\mathcal{L}\left(\mathbf{w}_2, \mathbf{u}, \mathbf{v}, \mathbf{c}\right) = \|\mathbf{w}_2\|^2 + \sum_{i=1}^{K} u_i \left(\mathbf{b}_i^T \mathbf{w}_2 - \bar{\mathbf{h}}_i^T \mathbf{w}_2 \tan \psi + \sqrt{\tilde{\Gamma}_i} \tan \psi\right)$$

$$+ \sum_{i=1}^{K} v_i \left(-\mathbf{b}_i^T \mathbf{w}_2 - \bar{\mathbf{h}}_i^T \mathbf{w}_2 \tan \psi + \sqrt{\tilde{\Gamma}_i} \tan \psi\right) + \sum_{m=1}^{M} c_m \left(\|\boldsymbol{\beta}_m^T \mathbf{w}_2\|^2 - R_m \sigma_R^2\right)$$

$$= \mathbf{w}_2^T \left(\mathbf{I} + \sum_{m=1}^{M} c_m \boldsymbol{\beta}_m \boldsymbol{\beta}_m^T\right) \mathbf{w}_2 + \sum_{i=1}^{K} \left[(u_i - v_i) \mathbf{b}_i^T - (u_i + v_i) \bar{\mathbf{h}}_i^T \tan \psi\right] \mathbf{w}_2 + \tan \psi \sum_{i=1}^{K} \sqrt{\tilde{\Gamma}_i} (u_i + v_i) - R_m \sigma_R^2 \sum_{m=1}^{M} c_m. \qquad (27)$$

D. Complexity Analysis

Note that the complexity of Algorithm 1 is mainly determined by the computation of the gradient (35), which needs to be done by each iteration. Here we measure the analytic complexity in terms of floating-point operation (flop), which is defined as one addition, subtraction, multiplication, or division of two floating-point numbers. Under such a definition, the complexity for computing (35) mainly lies in the matrix inverse operation, i.e., to calculate $\mathbf{M}$, which is $\mathcal{O}(N^3)$. Hence, the complexity for Algorithm 1 is $\mathcal{O}(N_{iter} N^3)$, where N_{iter} is the number of iterations, which is known to have the order of magnitude of $\mathcal{O}(\log(1/\varepsilon))$ [41], with ε being the stopping tolerance. For one communication frame that consists of L symbols, the total complexity for the beamforming problem will be $\mathcal{O}(LN_{iter} N^3)$. In contrast, for the semidefinite relaxation of $\mathcal{P}_0$, the corresponding SDP problem has K matrix variables of size $N \times N$, and $K + M$ linear constraints. The interior point method used in *SeDuMi* will take $\mathcal{O}(\sqrt{KN} \log(1/\varepsilon))$ iterations to convergence, with each iteration requiring at most $\mathcal{O}(K^3 N^6 + K(K + M)N^2)$ flops [42]. Considering that this is in fact an upper-bound of the complexity of the SDR beamforming problem, and the number of iterations N_{iter} for Algorithm 1 is unknown, we can conclude that the proposed Algorithm 1 will have at least the comparable complexity with its counterpart of SDR beamforming. This has been further verified via numerical simulations.

V. IMPACT ON RADAR PERFORMANCE

A. SDR Based Beamforming

The interference from BS to radar will have an impact on radar's performance, which will lower the detection probability and the accuracy for Direction of Arrival (DoA) estimation. First we consider the detection problem. Note that the target detection process can be described as a binary hypothesis testing problem, which is given by

$$
\mathbf{y}_l^R = \begin{cases} \mathcal{H}_1 : \alpha\sqrt{P_R}\mathbf{A}(\theta)\mathbf{s}_l + \mathbf{G}^T \sum_{k=1}^K \mathbf{t}_k d_k[l] + \mathbf{z}_l, \\ \qquad l = 1, 2, \dots, L, \\ \mathcal{H}_0 : \mathbf{G}^T \sum_{k=1}^K \mathbf{t}_k d_k[l] + \mathbf{z}_l, \quad l = 1, 2, \dots, L. \end{cases}
$$
(36)

For simplicity, we assume that the covariance matrix of the interference-plus-noise has been accurately estimated by the radar. Due to the unknown parameters α and θ, we use the Generalized Likelihood Ratio Test (GLRT) method to solve the above problem. Consider the sufficient statistic of the received signal, which is obtained by matched filtering [34], and is given by

$$
\tilde{\mathbf{Y}} = \frac{1}{\sqrt{L}} \sum_{l=1}^L \mathbf{y}_l^R \mathbf{s}_l^H
$$

$$
= \alpha\sqrt{LP_R}\mathbf{A}(\theta) + \frac{1}{\sqrt{L}} \sum_{l=1}^L \left(\mathbf{G}^T \sum_{k=1}^K \mathbf{t}_k d_k[l] + \mathbf{z}_l \right) \mathbf{s}_l^H.
$$
(37)

Let $\tilde{\mathbf{y}}$ be the vectorization of $\tilde{\mathbf{Y}}$, we have

$$
\tilde{\mathbf{y}} = \text{vec}\left(\tilde{\mathbf{Y}}\right) = \alpha\sqrt{LP_R} \, \text{vec}\left(\mathbf{A}(\theta)\right)
$$

$$
+ \text{vec}\left(\frac{1}{\sqrt{L}} \sum_{l=1}^L \left(\mathbf{G}^T \sum_{k=1}^K \mathbf{t}_k d_k[l] + \mathbf{z}_l \right) \mathbf{s}_l^H \right)
$$

$$
\triangleq \alpha\sqrt{LP_R} \, \text{vec}\left(\mathbf{A}(\theta)\right) + \boldsymbol{\varepsilon},
$$
(38)

where $\boldsymbol{\varepsilon}$ is zero-mean, complex Gaussian distributed, and has the following block covariance matrix as

$$
\mathbf{C} = \begin{bmatrix} \mathbf{J} + \sigma_R^2 \mathbf{I}_M & & \mathbf{0} \\ & \dots & \\ \mathbf{0} & & \mathbf{J} + \sigma_R^2 \mathbf{I}_M \end{bmatrix},
$$
(39)

where $\mathbf{C} \in \mathbb{C}^{M^2 \times M^2}$, and $\mathbf{J} = \mathbf{G}^T \sum_{k=1}^K \mathbf{t}_k \mathbf{t}_k^H \mathbf{G}^*$.

In [34], the GLRT detection is derived in the presence of white noise only. As shown above, $\boldsymbol{\varepsilon}$ is also Gaussian distributed and has a non-white covariance matrix. Hence we apply a whitening filter for the case. It is easy to verify that $\mathbf{C}$ and $\mathbf{C}^{-1}$ are both positive-definite Hermitian matrices. We then consider the Chelosky decomposition of $\mathbf{C}^{-1}$, i.e., $\mathbf{C}^{-1} = \mathbf{U}\mathbf{U}^H$, where $\mathbf{U}$ is a lower triangle matrix. By using $\mathbf{U}^H$ as a whitening filter, (36) can be reformulated as

$$
\tilde{\mathbf{y}}_w = \begin{cases} \mathcal{H}_1 : \alpha\sqrt{LP_R}\mathbf{U}^H\mathbf{d}(\theta) + \mathbf{U}^H\boldsymbol{\varepsilon}, \\ \mathcal{H}_0 : \mathbf{U}^H\boldsymbol{\varepsilon}, \end{cases}
$$
(40)

where $\mathbf{U}^H\boldsymbol{\varepsilon} \sim \mathcal{CN}(0, \mathbf{I}_{M^2})$. As per the standard GLRT decision rule, if

$$
L_{\tilde{\mathbf{y}}}\left(\hat{\alpha}, \hat{\theta}\right) = \frac{p\left(\tilde{\mathbf{y}}; \hat{\alpha}, \hat{\theta}, \mathcal{H}_1\right)}{p\left(\tilde{\mathbf{y}}; \mathcal{H}_0\right)} > \eta,
$$
(41)

then $\mathcal{H}_1$ is chosen, where $p(\tilde{\mathbf{y}}; \hat{\alpha}, \hat{\theta}, \mathcal{H}_1)$ and $p(\tilde{\mathbf{y}}; \mathcal{H}_0)$ are the Probability Density Function (PDF) under $\mathcal{H}_1$ and $\mathcal{H}_0$ respectively, $\hat{\alpha}$ and $\hat{\theta}$ is the maximum likelihood estimation (MLE) of α and θ under $\mathcal{H}_1$, and is given by $[\hat{\alpha}, \hat{\theta}] = \max_{\alpha, \theta} p(\tilde{\mathbf{y}}|\alpha, \theta, \mathcal{H}_1)$, η is the decision threshold. According to [43], for a given θ, the MLE of α is given by the complex least-squares (LS) estimation, which is

$$
\hat{\alpha} = \frac{\mathbf{d}^H(\theta)\mathbf{C}^{-1}\tilde{\mathbf{y}}}{\mathbf{d}^H(\theta)\mathbf{C}^{-1}\mathbf{d}(\theta)}.
$$
(42)

By substituting (42) into (41), and taking the logarithm at both sides, the MLE of θ is given as

$$
\hat{\theta} = \arg\max_{\theta} \frac{\left| \mathbf{d}^H(\theta)\mathbf{C}^{-1}\tilde{\mathbf{y}} \right|^2}{\mathbf{d}^H(\theta)\mathbf{C}^{-1}\mathbf{d}(\theta)}.
$$
(43)

Hence, the GLRT test statistic is given by

$$
\ln L_{\tilde{\mathbf{y}}}\left(\hat{\theta}\right) = \frac{\left| \mathbf{d}^H(\hat{\theta})\mathbf{U}\mathbf{U}^H\tilde{\mathbf{y}} \right|^2}{\left\| \mathbf{U}^H\mathbf{d}(\hat{\theta}) \right\|^2} = \frac{\left| \mathbf{d}^H(\hat{\theta})\mathbf{C}^{-1}\tilde{\mathbf{y}} \right|^2}{\mathbf{d}^H(\hat{\theta})\mathbf{C}^{-1}\mathbf{d}(\hat{\theta})}
$$

$$
= \frac{\left| \text{tr}\left(\tilde{\mathbf{Y}}\mathbf{A}^H(\hat{\theta})\tilde{\mathbf{J}}^{-1}\right) \right|^2}{\text{tr}\left(\mathbf{A}(\hat{\theta})\mathbf{A}^H(\hat{\theta})\tilde{\mathbf{J}}^{-1}\right)} \underset{\mathcal{H}_0}{\overset{\mathcal{H}_1}{\gtrless}} \eta,
$$
(44)

where $\tilde{\mathbf{J}} = \mathbf{J} + \sigma_R^2 \mathbf{I}_M$. According to [44], the asymptotic distribution of (44) is given by

$$\ln L_{\tilde{\mathbf{y}}}\left(\hat{\theta}\right) \sim \begin{cases} \mathcal{H}_1 : \mathcal{X}_2^2\left(\rho\right), \\ \mathcal{H}_0 : \mathcal{X}_2^2, \end{cases} \quad (45)$$

where $\mathcal{X}_2^2$ and $\mathcal{X}_2^2(\rho)$ are central and non-central chi-squared distributions with two Degrees of Freedom (DoFs), and ρ is the non-central parameter, which is given by

$$\rho = |\alpha|^2 L P_R \text{vec}^H\left(\mathbf{A}\left(\theta\right)\right) \mathbf{C}^{-1} \text{vec}\left(\mathbf{A}\left(\theta\right)\right)$$
$$= \text{SNR}_R \sigma_R^2 \, \text{tr}\left(\mathbf{A}\left(\theta\right) \mathbf{A}^H\left(\theta\right)\left(\mathbf{J} + \sigma_R^2 \mathbf{I}_M\right)^{-1}\right), \quad (46)$$

where we define radar SNR as $\text{SNR}_R = \frac{|\alpha|^2 L P_R}{\sigma_R^2}$ [34]. To maintain a constant false alarm rate P_{FA}, η is decided by the given P_{FA} under Neyman-Pearson criterion [44], i.e.,

$$P_{FA} = 1 - \mathfrak{F}_{\mathcal{X}_2^2}\left(\eta\right), \eta = \mathfrak{F}_{\mathcal{X}_2^2}^{-1}\left(1 - P_{FA}\right), \quad (47)$$

where $\mathfrak{F}_{\mathcal{X}_2^2}^{-1}$ is the inverse function of chi-squared Cumulative Distribution Function (CDF) with 2 DoFs. The detection probability is thus given as

$$P_D = 1 - \mathfrak{F}_{\mathcal{X}_2^2(\rho)}(\eta) = 1 - \mathfrak{F}_{\mathcal{X}_2^2(\rho)}\left(\mathfrak{F}_{\mathcal{X}_2^2}^{-1}\left(1 - P_{FA}\right)\right), \quad (48)$$

where $\mathfrak{F}_{\mathcal{X}_2^2(\rho)}$ is the non-central chi-squared CDF with 2 DoFs.

It is well-known that the accuracy of parameter estimation can be measured by the Cramér-Rao bound [45], which is the lower bound for all the unbiased estimators. In our case, the parameters to be estimated are θ and α. The Fisher Information matrix is partitioned as

$$\boldsymbol{\xi}\left(\tilde{\mathbf{y}}\right) = \begin{bmatrix} \xi_{\theta\theta} & \boldsymbol{\xi}_{\theta\alpha}^T \\ \boldsymbol{\xi}_{\theta\alpha} & \boldsymbol{\xi}_{\alpha\alpha} \end{bmatrix}, \quad (49)$$

where $\xi_{\theta\theta}$ is a scalar, $\boldsymbol{\xi}_{\theta\alpha}$ is a vector and $\boldsymbol{\xi}_{\alpha\alpha}$ is a matrix for the reason that θ is a real parameter while α is complex. The CRB for DoA estimation is given by

$$\text{CRB}\left(\theta\right) = \left(\xi_{\theta\theta} - \boldsymbol{\xi}_{\theta\alpha}^T \boldsymbol{\xi}_{\alpha\alpha}^{-1} \boldsymbol{\xi}_{\theta\alpha}\right)^{-1}. \quad (50)$$

By the similar derivation as [34], $\xi_{\theta\theta}, \boldsymbol{\xi}_{\alpha\alpha}$ and $\boldsymbol{\xi}_{\theta\alpha}$ are given as

$$\xi_{\theta\theta} = 2|\alpha|^2 L P_R \, \text{tr}\left(\dot{\mathbf{A}}\left(\theta\right) \dot{\mathbf{A}}^H\left(\theta\right) \tilde{\mathbf{J}}^{-1}\right),$$

$$\boldsymbol{\xi}_{\alpha\alpha} = 2 L P_R \, \text{tr}\left(\mathbf{A}\left(\theta\right) \mathbf{A}^H\left(\theta\right) \tilde{\mathbf{J}}^{-1}\right) \mathbf{I}_2,$$

$$\boldsymbol{\xi}_{\theta\alpha} = 2 L P_R \, \text{Re}\left(\alpha^* \text{tr}\left(\mathbf{A}\left(\theta\right) \dot{\mathbf{A}}^H\left(\theta\right) \tilde{\mathbf{J}}^{-1}\right)(1; j)\right), \quad (51)$$

where $\dot{\mathbf{A}}(\theta) = \frac{\partial \mathbf{A}(\theta)}{\partial \theta}$. By substituting (51) into (50), we have

$$\text{CRB}\left(\theta\right)$$
$$= \frac{1}{2\text{SNR}_R \sigma_R^2} \cdot$$
$$\frac{\text{tr}\left(\mathbf{A}\mathbf{A}^H \tilde{\mathbf{J}}^{-1}\right)}{\text{tr}\left(\dot{\mathbf{A}}\dot{\mathbf{A}}^H \tilde{\mathbf{J}}^{-1}\right) \text{tr}\left(\mathbf{A}\mathbf{A}^H \tilde{\mathbf{J}}^{-1}\right) - \left|\text{tr}\left(\mathbf{A}\dot{\mathbf{A}}^H \tilde{\mathbf{J}}^{-1}\right)\right|^2}, \quad (52)$$

B. Constructive Interference Based Beamforming

The proposed CI-based beamforming should be computed symbol by symbol, which means that the precoding vectors are functions of the time index, thus the corresponding hypothesis testing problem (36) is modified as

$$\mathbf{y}_l^R = \begin{cases} \mathcal{H}_1 : \alpha\sqrt{P_R}\mathbf{A}\left(\theta\right)\mathbf{s}_l + \mathbf{G}^T\tilde{\mathbf{w}}[l] + \mathbf{z}_l, \\ \quad\quad l = 1, 2, \dots, L, \\ \mathcal{H}_0 : \mathbf{G}^T\tilde{\mathbf{w}}[l] + \mathbf{z}_l, \quad l = 1, 2, \dots, L, \end{cases} \quad (53)$$

where $\tilde{\mathbf{w}}[l] = \mathbf{w}[l]e^{j\phi_1[l]}$. While the exact analytic form of the distribution for $\mathbf{w}[l]$ is hard to derive, here we employ the Gaussian detector for SDR beamformer in (44). We note that for CI precoding, $\mathbf{w}[l]$ is not in general Gaussian. Nevertheless, since each element of $\mathbf{G}^T\mathbf{w}[l]$ can be viewed as the linear combination of multiple random variables within one channel realization, the resultant interference subjects to Gaussian distribution approximately according to the central-limit theorem. Our numerical results show that this is indeed an affordable approximation, and, even with a Gaussian detector, CI-based beamformer achieves better performance at radar. Following the same procedure of the previous subsection, we have

$$\mathbf{J} = \frac{1}{L}\sum_{l=1}^L \mathbf{G}^T\tilde{\mathbf{w}}[l]\tilde{\mathbf{w}}^H[l]\mathbf{G}^* = \frac{1}{L}\sum_{l=1}^L \mathbf{G}^T\mathbf{w}[l]\mathbf{w}^H[l]\mathbf{G}^*. \quad (54)$$

By substituting (54) into (48) and (52) we obtain the approximated detection probability and the $\text{CRB}(\theta)$ of CI-based beamforming method.

VI. ROBUST BEAMFORMING FOR POWER MINIMIZATION WITH BOUNDED CSI ERRORS

A. Channel Error Model

It is generally difficult to obtain perfect CSI in the practical scenarios. In this section, we study the beamforming design for imperfect CSI. Following the standard assumptions in the related literatures, let us first model the channel vectors as

$$\mathbf{h}_i = \hat{\mathbf{h}}_i + \mathbf{e}_{hi}, \mathbf{f}_i = \hat{\mathbf{f}}_i + \mathbf{e}_{fi}, \forall i,$$
$$\mathbf{g}_m = \hat{\mathbf{g}}_m + \mathbf{e}_{gm}, \forall m, \quad (55)$$

where $\hat{\mathbf{h}}_i, \hat{\mathbf{g}}_m$ and $\hat{\mathbf{f}}_i$ denote the estimated channel vectors known to the BS, $\mathbf{e}_{hi}, \mathbf{e}_{gm}$ and $\mathbf{e}_{fi}$ denote the CSI uncertainty within the spherical sets $\mathcal{U}_{hi} = \{\mathbf{e}_{hi}|\|\mathbf{e}_{hi}\|^2 \leq \delta_{hi}^2\}$, $\mathcal{U}_{gm} = \{\mathbf{e}_{gm}| \|\mathbf{e}_{gm}\|^2 \leq \delta_{gm}^2\}$ and $\mathcal{U}_{fi} = \{\mathbf{e}_{fi}|\|\mathbf{e}_{fi}\|^2 \leq \delta_{fi}^2\}$. This model is reasonable for scenarios that CSI is quantized at the receiver and fed back to the BS. Particularly, if the quantizer is uniform, the quantization error region can be covered by spheres of given sizes [46].

It is assumed that BS has no knowledge about the error vectors except for the bounds of their norms. We therefore consider a worst-case approach to guarantee the solution is robust to all the uncertainties in above spherical sets. It should be highlighted that this is only valid when all the uncertainties lie in the constraints. For the interference minimization problem, we can not formulate a robust problem in the real sense because

the uncertainty of the channel $\mathbf{G}$ lies in the objective function. However, a weighting minimization method can be applied for the case to obtain a suboptimal result. Readers are referred to [18] for details. Due to the limited space, we designate this as the objective of the future work, and focus on the robust version for power minimization in this paper.

B. SDR Based Robust Beamforming

The robust version of the SDR-based problem $\mathcal{P}_0$ is given by

$$\mathcal{P}_9 : \min_{\mathbf{t}_k} \quad \sum_{k=1}^{K} \|\mathbf{t}_k\|^2$$

$$s.t. \quad \frac{\left|\mathbf{h}_i^T \mathbf{t}_i\right|^2}{\sum_{k=1, k\neq i}^{K} \left|\mathbf{h}_i^T \mathbf{t}_k\right|^2 + P_R \|\mathbf{f}_i\|^2 + \sigma_C^2} \geq \Gamma_i$$

$$\forall \mathbf{e}_{hi} \in \mathcal{U}_{hi}, \forall \mathbf{e}_{fi} \in \mathcal{U}_{fi}, \forall i,$$

$$\left|\mathbf{g}_m^T \sum_{k=1}^{K} \mathbf{t}_k d_k\right|^2 \leq R_m \sigma_R^2, \forall \mathbf{e}_{gm} \in \mathcal{U}_{gm}, \forall m. \quad (56)$$

The above problem is then reformulated as a worst-case approach, and can be solved by employing the well-known S-procedure [38]. According to basic linear algebra, we have

$$\|\mathbf{f}_i\|^2 = \left\|\hat{\mathbf{f}}_i + \mathbf{e}_{fi}\right\|^2 \leq \left(\left\|\hat{\mathbf{f}}_i\right\| + \|\mathbf{e}_{fi}\|\right)^2 \leq \left(\left\|\hat{\mathbf{f}}_i\right\| + \delta_{fi}\right)^2. \quad (57)$$

Similarly, for the interference power we have

$$\left|\mathbf{g}_m^T \sum_{k=1}^{K} \mathbf{t}_k d_k\right|^2 = \sum_{k=1}^{K} \mathrm{tr}\left((\hat{\mathbf{g}}_m^* + \mathbf{e}_{gm}^*)(\hat{\mathbf{g}}_m^T + \mathbf{e}_{gm}^T)\mathbf{t}_k \mathbf{t}_k^H\right)$$

$$= \sum_{k=1}^{K} \mathrm{tr}\left((\hat{\mathbf{g}}_m^* \hat{\mathbf{g}}_m^T + \hat{\mathbf{g}}_m^* \mathbf{e}_{gm}^T + \mathbf{e}_m^* \hat{\mathbf{g}}_m^T + \mathbf{e}_{gm}^* \mathbf{e}_{gm}^T)\mathbf{t}_k \mathbf{t}_k^H\right). \quad (58)$$

By using the Cauchy-Schwarz inequality and rearranging the formula, it follows that

$$\left|\mathbf{g}_m^* \sum_{k=1}^{K} \mathbf{t}_k d_k\right|^2 \leq \sum_{k=1}^{K} \mathrm{tr}\left(\hat{\mathbf{g}}_m^* \hat{\mathbf{g}}_m^T \mathbf{t}_k \mathbf{t}_k^H\right)$$

$$+ \left(2\|\hat{\mathbf{g}}_m\|\|\mathbf{e}_{gm}\| + \|\mathbf{e}_{gm}\|^2\right)\sum_{k=1}^{K} \mathrm{tr}\left(\mathbf{t}_k \mathbf{t}_k^H\right)$$

$$\leq \sum_{k=1}^{K} \mathrm{tr}\left(\hat{\mathbf{g}}_m^* \hat{\mathbf{g}}_m^T \mathbf{t}_k \mathbf{t}_k^H\right) + \left(2\delta_{gm}\|\hat{\mathbf{g}}_m\| + \delta_{gm}^2\right)\sum_{k=1}^{K} \mathrm{tr}\left(\mathbf{t}_k \mathbf{t}_k^H\right). \quad (59)$$

Based on the work [18], we directly give the worst-case formulation of $\mathcal{P}_9$ by

$$\mathcal{P}_{10} : \min_{\mathbf{T}_i, s_i} \sum_{i=1}^{K} \mathrm{tr}(\mathbf{T}_i)$$

$$s.t. \begin{bmatrix} \hat{\mathbf{h}}_i^T \mathbf{Q}_i \hat{\mathbf{h}}_i^* - \Gamma_i \beta_i - s_i \delta_{hi}^2 & \hat{\mathbf{h}}_i^T \mathbf{Q}_i \\ \mathbf{Q}_i \hat{\mathbf{h}}_i^* & \mathbf{Q}_i + s_i \mathbf{I} \end{bmatrix} \succeq 0,$$

$$\mathbf{T}_i \succeq 0, \mathbf{T}_i = \mathbf{T}_i^*, \mathrm{rank}(\mathbf{T}_i) = 1, s_i \geq 0, \forall i,$$

$$\sum_{i=1}^{K} \left(\mathrm{tr}(\hat{\mathbf{g}}_m^* \hat{\mathbf{g}}_m^T \mathbf{T}_i) + \zeta_{gm} \mathrm{tr}(\mathbf{T}_i)\right) \leq R_m \sigma_R^2, \forall m, \quad (60)$$

where $\mathbf{T}_k = \mathbf{t}_k \mathbf{t}_k^H$, $\mathbf{Q}_i = \mathbf{T}_i - \Gamma_i \sum_{n=1, n\neq i}^{K} \mathbf{T}_n$, $\zeta_{gm} = 2\delta_2 \|\hat{\mathbf{g}}_m\| + \delta_{gm}^2$ and $\beta_i = P_R(\|\hat{\mathbf{f}}_i\| + \delta_{fi})^2 + \sigma_C^2$. By dropping the rank constraint on $\mathbf{T}_i$, the above problem becomes a standard SDP and can be solved by SDR method, after which the beamforming vectors can be obtained by rank-1 approximation or Gaussian randomization [19].

C. Constructive Interference Based Robust Beamforming

Let us first formulate the robust version of the virtual multicast problem $\mathcal{P}_4$ as

$$\mathcal{P}_{11} : \min_{\mathbf{w}} \quad \|\mathbf{w}\|^2$$

$$s.t. \left|\mathrm{Im}\left(\tilde{\mathbf{h}}_i^T \mathbf{w}\right)\right| \leq \left(\mathrm{Re}\left(\tilde{\mathbf{h}}_i^T \mathbf{w}\right) - \sqrt{\tilde{\Gamma}_i}\right)\tan\psi,$$

$$\forall \mathbf{e}_{hi} \in \mathcal{U}_{hi}, \forall \mathbf{e}_{fi} \in \mathcal{U}_{fi}, \forall i,$$

$$\left|\tilde{\mathbf{g}}_m^T \mathbf{w}\right| \leq \sqrt{R_m \sigma_R^2}, \forall \mathbf{e}_{gm} \in \mathcal{U}_{gm}, \forall m. \quad (61)$$

Similar to (57), the robust case for the channel vector $\mathbf{f}_i$ can be given as

$$\left|\mathbf{f}_i^T \mathbf{s}\right|^2 = \left|\hat{\mathbf{f}}_i^T \mathbf{s} + \mathbf{e}_{fi}^T \mathbf{s}\right|^2$$

$$\leq \left(\left|\hat{\mathbf{f}}_i^T \mathbf{s}\right| + \left|\mathbf{e}_{fi}^T \mathbf{s}\right|\right)^2 \leq \left(\left|\hat{\mathbf{f}}_i^T \mathbf{s}\right| + \delta_{fi}\|\mathbf{s}\|\right)^2. \quad (62)$$

Consider the worst case of the INR constraints, which is

$$\max \quad \left|\tilde{\mathbf{g}}_m^T \mathbf{w}\right| \leq \sqrt{R_m \sigma_R^2}, \forall \mathbf{e}_{gm} \in \mathcal{U}_{gm}, \forall m. \quad (63)$$

Since $\tilde{\mathbf{g}}_m \triangleq \mathbf{g}_m e^{j\phi_1}$, it is easy to see $\|\tilde{\mathbf{g}}_m \mathbf{w}\|^2 = \|\mathbf{g}_m \mathbf{w}\|^2$. For the convenience of further analysis, we drop the subscript, and denote the interference channel vector by its real and imaginary parts, which is given by

$$\mathbf{g} = \hat{\mathbf{g}}_R + j\hat{\mathbf{g}}_I + \mathbf{e}_{gR} + j\mathbf{e}_{gI}. \quad (64)$$

Let $\bar{\mathbf{g}} = [\hat{\mathbf{g}}_R; \hat{\mathbf{g}}_I], \bar{\mathbf{e}}_g = [\mathbf{e}_{gR}; \mathbf{e}_{gI}]$, the interference from radar can be written as

$$\left|\tilde{\mathbf{g}}^T \mathbf{w}\right|^2 = \left\| \begin{bmatrix} \hat{\mathbf{g}}_R^T + \mathbf{e}_{gR}^T & \hat{\mathbf{g}}_I^T + \mathbf{e}_{gI}^T \\ \hat{\mathbf{g}}_I^T + \mathbf{e}_{gI}^T & -\hat{\mathbf{g}}_R^T - \mathbf{e}_{gR}^T \end{bmatrix} \begin{bmatrix} \mathbf{w}_R \\ -\mathbf{w}_I \end{bmatrix} \right\|^2$$

$$= \left\| \begin{matrix} \bar{\mathbf{g}}^T \mathbf{w}_2 + \bar{\mathbf{e}}_g^T \mathbf{w}_2 \\ \bar{\mathbf{g}}^T \mathbf{w}_1 + \bar{\mathbf{e}}_g^T \mathbf{w}_1 \end{matrix} \right\|^2, \tag{65}$$

According to the Cauchy-Schwarz inequality, (65) can be further expanded as

$$\left\| \begin{matrix} \bar{\mathbf{g}}^T \mathbf{w}_2 + \bar{\mathbf{e}}_g^T \mathbf{w}_2 \\ \bar{\mathbf{g}}^T \mathbf{w}_1 + \bar{\mathbf{e}}_g^T \mathbf{w}_1 \end{matrix} \right\|^2$$

$$\leq \left|\bar{\mathbf{g}}^T \mathbf{w}_2\right|^2 + \left|\bar{\mathbf{g}}^T \mathbf{w}_1\right|^2 + 2\delta_g^2 \|\mathbf{w}_2\|^2$$

$$+ 2\delta_g \left(\left\|\bar{\mathbf{g}}^T \mathbf{w}_2 \mathbf{w}_2^T\right\| + \left\|\bar{\mathbf{g}}^T \mathbf{w}_1 \mathbf{w}_1^T\right\| \right)$$

$$\leq \left|\bar{\mathbf{g}}^T \mathbf{w}_2\right|^2 + \left|\bar{\mathbf{g}}^T \mathbf{w}_1\right|^2 + \left(2\delta_g^2 + 4\delta_g \|\bar{\mathbf{g}}\| \right) \|\mathbf{w}_2\|^2, \tag{66}$$

and the robust constraint for INR is given by

$$\left|\bar{\mathbf{g}}^T \mathbf{w}_2\right|^2 + \left|\bar{\mathbf{g}}^T \mathbf{w}_1\right|^2 + \left(2\delta_g^2 + 4\delta_g \|\bar{\mathbf{g}}\| \right) \|\mathbf{w}_2\|^2 \leq R\sigma_R^2. \tag{67}$$

For the SINR constraint, note that the corresponding worst case is equivalent to

$$\max \quad \left| \mathrm{Im}\left(\tilde{\mathbf{h}}_i^T \mathbf{w} \right) \right| - \mathrm{Re}\left(\tilde{\mathbf{h}}_i^T \mathbf{w} \right) \tan \psi + \sqrt{\tilde{\Gamma}_i} \tan \psi \leq 0,$$

$$\forall \mathbf{e}_{hi} \in \mathcal{U}_{hi}, \forall \mathbf{e}_{fi} \in \mathcal{U}_{fi}, \forall i. \tag{68}$$

Let $\hat{\tilde{\mathbf{h}}}_i = \hat{\mathbf{h}}_i e^{j(\phi_1 - \phi_i)}, \tilde{\mathbf{e}}_{hi} = \mathbf{e}_{hi} e^{j(\phi_1 - \phi_i)}$, we have $\tilde{\mathbf{h}}_i = \hat{\tilde{\mathbf{h}}}_i + \tilde{\mathbf{e}}_{hi}$. Similarly, we drop the subscript and denote the channel vector by its real and imaginary parts, which is

$$\tilde{\mathbf{h}} = \hat{\tilde{\mathbf{h}}}_R + j\hat{\tilde{\mathbf{h}}}_I + \tilde{\mathbf{e}}_{hR} + j\tilde{\mathbf{e}}_{hI}. \tag{69}$$

It follows that

$$\mathrm{Im}\left(\tilde{\mathbf{h}}\mathbf{w} \right) = \mathrm{Im}\left(\left(\hat{\tilde{\mathbf{h}}}_R + j\hat{\tilde{\mathbf{h}}}_I + \tilde{\mathbf{e}}_{hR} + j\tilde{\mathbf{e}}_{hI} \right) (\mathbf{w}_R + j\mathbf{w}_I) \right)$$

$$= \left[\hat{\tilde{\mathbf{h}}}_R, \hat{\tilde{\mathbf{h}}}_I \right] \begin{bmatrix} \mathbf{w}_I \\ \mathbf{w}_R \end{bmatrix} + \left[\tilde{\mathbf{e}}_{hR}, \tilde{\mathbf{e}}_{hI} \right] \begin{bmatrix} \mathbf{w}_I \\ \mathbf{w}_R \end{bmatrix}$$

$$\triangleq \hat{\tilde{\mathbf{h}}}^T \mathbf{w}_1 + \bar{\mathbf{e}}_h^T \mathbf{w}_1, \tag{70}$$

$$\mathrm{Re}\left(\tilde{\mathbf{h}}\mathbf{w} \right) = \mathrm{Re}\left(\left(\hat{\tilde{\mathbf{h}}}_R + j\hat{\tilde{\mathbf{h}}}_I + \tilde{\mathbf{e}}_{hR} + j\tilde{\mathbf{e}}_{hI} \right) (\mathbf{w}_R + j\mathbf{w}_I) \right)$$

$$= \left[\hat{\tilde{\mathbf{h}}}_R, \hat{\tilde{\mathbf{h}}}_I \right] \begin{bmatrix} \mathbf{w}_R \\ -\mathbf{w}_I \end{bmatrix} + \left[\tilde{\mathbf{e}}_{hR}, \tilde{\mathbf{e}}_{hI} \right] \begin{bmatrix} \mathbf{w}_R \\ -\mathbf{w}_I \end{bmatrix}$$

$$\triangleq \hat{\tilde{\mathbf{h}}}^T \mathbf{w}_2 + \bar{\mathbf{e}}_h^T \mathbf{w}_2. \tag{71}$$

By noting that $\|\bar{\mathbf{e}}_h\|^2 \leq \delta_h^2$, (68) is equivalent to

$$\max \left| \hat{\tilde{\mathbf{h}}}^T \mathbf{w}_1 + \bar{\mathbf{e}}_h^T \mathbf{w}_1 \right| - \left(\hat{\tilde{\mathbf{h}}}^T \mathbf{w}_2 + \bar{\mathbf{e}}_h^T \mathbf{w}_2 \right) \tan \psi$$

$$+ \sqrt{\tilde{\Gamma}} \tan \psi \leq 0, \forall \|\bar{\mathbf{e}}_h\|^2 \leq \delta_h^2, \forall \|\mathbf{e}_f\|^2 \leq \delta_f^2, \tag{72}$$

and can be decomposed into the following two constraints:

$$\max \hat{\tilde{\mathbf{h}}}^T \mathbf{w}_1 + \bar{\mathbf{e}}_h^T \mathbf{w}_1 - \left(\hat{\tilde{\mathbf{h}}}^T \mathbf{w}_2 + \bar{\mathbf{e}}_h^T \mathbf{w}_2 \right) \tan \psi$$

$$+ \sqrt{\tilde{\Gamma}} \tan \psi \leq 0, \forall \|\bar{\mathbf{e}}_h\|^2 \leq \delta_h^2, \forall \|\mathbf{e}_f\|^2 \leq \delta_f^2, \tag{73}$$

$$\max -\hat{\tilde{\mathbf{h}}}^T \mathbf{w}_1 - \bar{\mathbf{e}}_h^T \mathbf{w}_1 - \left(\hat{\tilde{\mathbf{h}}}^T \mathbf{w}_2 + \bar{\mathbf{e}}_h^T \mathbf{w}_2 \right) \tan \psi$$

$$+ \sqrt{\tilde{\Gamma}} \tan \psi \leq 0, \forall \|\bar{\mathbf{e}}_h\|^2 \leq \delta_h^2, \forall \|\mathbf{e}_f\|^2 \leq \delta_f^2. \tag{74}$$

Based on above, the worst-case constraints for (73) and (74) are given by

$$\hat{\tilde{\mathbf{h}}}^T \mathbf{w}_1 - \hat{\tilde{\mathbf{h}}}^T \mathbf{w}_2 \tan \psi + \delta_h \left(\mathbf{w}_1 - \mathbf{w}_2 \tan \psi \right)$$

$$+ \sqrt{\Gamma \left(\sigma_C^2 + P_R \left(\left|\hat{\mathbf{f}}^T \mathbf{s}\right| + \delta_f \|\mathbf{s}\| \right)^2 \right)} \tan \psi \leq 0, \tag{75}$$

$$-\hat{\tilde{\mathbf{h}}}^T \mathbf{w}_1 - \hat{\tilde{\mathbf{h}}}^T \mathbf{w}_2 \tan \psi + \delta_h \left(\mathbf{w}_1 + \mathbf{w}_2 \tan \psi \right)$$

$$+ \sqrt{\Gamma \left(\sigma_C^2 + P_R \left(\left|\hat{\mathbf{f}}^T \mathbf{s}\right| + \delta_f \|\mathbf{s}\| \right)^2 \right)} \tan \psi \leq 0. \tag{76}$$

The final robust optimization problem is given by

$$\mathcal{P}_{12} : \min_{\mathbf{w}_1} \quad \|\mathbf{w}_1\|^2$$

$$s.t. \quad \text{Constraints (67), (75) and (76)}, \forall i, \forall m,$$

$$\mathbf{w}_1 = \mathbf{\Pi} \mathbf{w}_2. \tag{77}$$

VII. NUMERICAL RESULTS

In this section, numerical results based on Monte Carlo simulations are shown to validate the effectiveness of the proposed beamforming method. Without loss of generality, we assume that $P_R = \frac{10}{M}$ kW, which results in a total transmit power of 10 kW for radar. The channel vectors are assumed to subject to complex Gaussian distributions, i.e., $\mathbf{h}_i \sim \mathcal{CN}(0, \rho_1^2 \mathbf{I}), \mathbf{f}_i \sim \mathcal{CN}(0, \rho_2^2 \mathbf{I}), \forall i, \mathbf{g}_m \sim \mathcal{CN}(0, \rho_3^2 \mathbf{I}), \forall m$, where $\rho_1 = 1, \rho_2 = \rho_3 = 2 \times 10^{-3}$. In this case, the distance from radar to the BS is hundreds of times of the distance between the BS and users. This is a typical coexistence scenario where an air traffic control (ATC) radar is located in the suburb area, and the BSs are located in the central city [47], [48]. Since the radar and the BS are operated in the same frequency band, we assume $\sigma_R^2 = \sigma_C^2 = 10^{-4}$. For simplicity, the INR thresholds for different radar antennas and the SINR level for different downlink users are set to be equal, respectively, i.e., $R_m = R, \Gamma_i = \Gamma, \forall i, \forall m$. For the robust cases, we set the normalized error bounds as $\delta_{hi}/\rho_1 = \delta_{fi}/\rho_2 = \delta_{gm}/\rho_3 = \delta, \forall i, \forall m$. While it is plausible that the benefits of the proposed scheme extend to various scenarios, here we assume $N = 10, K = M = 5$ unless otherwise specified, and explore the results for QPSK and 8PSK modulations. We denote the conventional SDR beamformer as 'SDR' in the figures, and the proposed beamformer based on constructive interference as 'CI'.
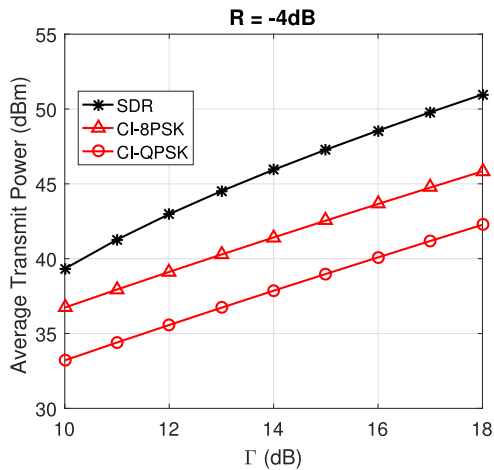
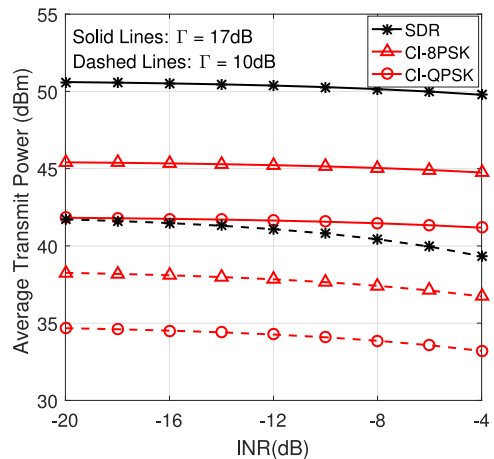Fig. 3. Average transmit power vs. required SINR, with $R = -4$ dB.

Fig. 4. Trade-off between BS transmit power and INR level, with $\Gamma = 10$ dB and 17 dB, respectively.
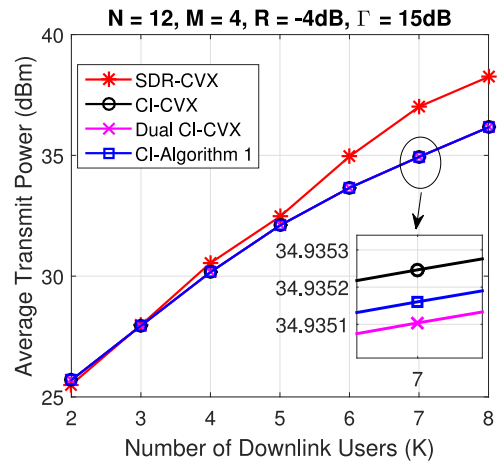

Fig. 5. Results comparison of Algorithm 1 and CVX-Solver for CI and SDR, $N = 12$, $M = 4$, $\Gamma = 15$ dB, and $R = -4$ dB, QPSK.
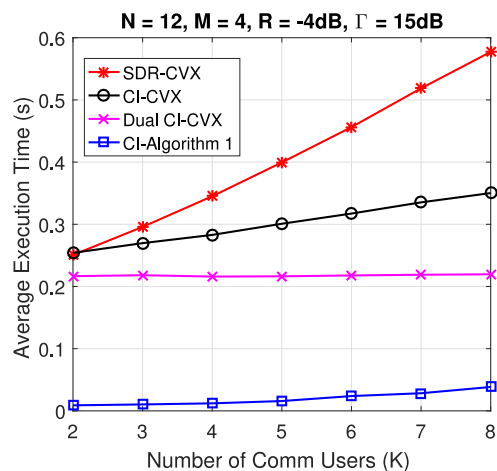

Fig. 6. Average execution time for optimization $\mathcal{P}_0$, $\mathcal{P}_3$ and Algorithm 1, $N = 12$, $M = 4$, $\Gamma = 15$ dB, and $R = -4$ dB, QPSK.

A. Average Transmit Power

In Fig. 3, we compare the minimized power for the two beam-forming methods under a given INR level of -4 dB with the increasing Γ. Unsurprisingly, the power needed for transmission increases with growing Γ for both methods. However, it can be easily seen that the proposed method obtains a lower transmit power for given INR and SINR requirements than the conventional SDR-based method thanks to the exploitation of the constructive interference. Particularly if QPSK modulation is used, the required power for CI-based scheme is less than half of the power needed for SDR-based beamforming. Furthermore, a 3 dB power-saving can be also observed for CI-QPSK compared to CI-8PSK. This is because the constructive region for QPSK is twice larger than the latter, leading to a more relaxed feasible region for the CI optimizations. Similar results have been provided in Fig. 4, where the transmit power of different methods with increased R has been given with required SINR fixed at 10 dB and 17 dB respectively. It is worth noting that there exists a trade-off between the power needed for BS and the INR level received by radar as has been discussed in the previous section. For both figures, we see that CI methods lead

to a practical BS transmit power that is less than 46 dBm, while the SDR beamformer requires up to 50 dBm (100W) to obtain the same SINR levels, which is far from realistic scenarios.

B. Efficent Algorithm

In order to verify the effectiveness of the proposed efficient algorithm for $\mathcal{P}_3$, we compare the results obtained by the built-in *SeDuMi* solver in CVX [49] and Algorithm 1 with increasing downlink users K in Fig. 5, where $N = 12$, $M = 4$, $\Gamma = 15$ dB, $R = -4$ dB. The required transmit power for SDR optimization $\mathcal{P}_0$ and the dual CI problem $\mathcal{P}_8$ using CVX solver is also presented as benchmarks. As we can see that the three CI curves match very well and the difference is less than 0.002 dBm when $M = 7$, and as expected, all the CI methods outperforms the SDR approach.

In Fig. 6, the complexities for the above 4 approaches in Fig. 5 have been compared in terms of average execution time for a growing number of downlink users, where all the configurations remain the same. Note that it takes less time to solve both the primal CI problem $\mathcal{P}_3$ and its dual $\mathcal{P}_8$ than the SDR optimization
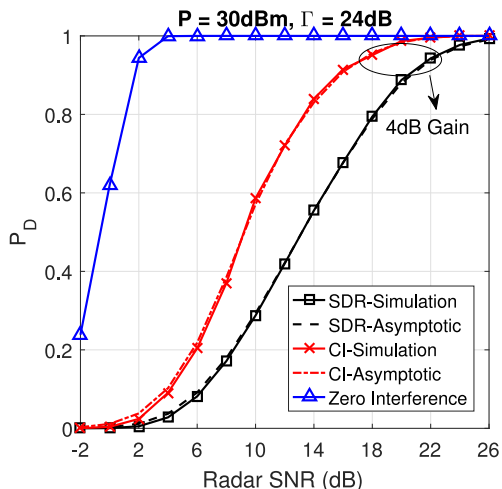
Fig. 7.　Detection probability vs. radar SNR for different cases, $P = 30$ dBm, $\Gamma = 24$ dB, $\eta = 13.5$ dBm, QPSK.

Fig. 8.　Detection Probability vs. SINR threshold for different cases, $P = 25$ dBm, QPSK.

$\mathcal{P}_0$ by the CVX solver. This is because to solve $\mathcal{P}_0$, an eigenvalue decomposition or Gaussian randomization is required to obtain the beamforming vectors, which involves extra amount of computations [19]. Nevertheless, the proposed CI-based approach is a symbol-level beamformer, which means that the beamforming vectors should be calculated symbol by symbol while the SDR-based beamforming needs only one-time calculation during a communication frame in slow fading channels. Fortunately, the proposed Algorithm 1 is far more efficient than the CVX solver, which needs only 6.7% of the time of the SDR optimization when $K = 8$. In a typical LTE system with 20 symbols in one frame, the total execution time for Algorithm 1 will be 134% ($6.7\% \times 20 = 134\%$) of the SDR-based beamforming, but the gain of the saved transmit power is more than 200% as has been shown in Figs. 3 and 4, which is cost-effective in energy-limited systems.

C. Radar Performance

Figs. 7–9 demonstrate a series of results for the impact of the proposed scheme on different radar metrics by solving the interference minimization problem $\mathcal{P}_2$ and $\mathcal{P}_5$. Here we assume that radar is equipped with a Uniform Linear Array (ULA) with half-wavelength spacing, and m-sequences are used as the radar waveform with a length of 50 digits, i.e., $L = 50$. The target is set to be located at the direction of $\theta = \pi/5$. In Fig. 7, the average detection probability with increased radar SNR for the two methods are given, where the solid line with triangle markers denotes the case without interference from the BS. Among the rest lines, the solid curves and dashed ones denote the simulated and asymptotic detection performance respectively. The parameters are given as $\eta = 13.5$ dBm, $\Gamma = 24$ dB, and $P = 30$ dBm. As shown in the figure, the simulated results match well with the asymptotic ones for both SDR and CI methods. Once again, we see that the proposed method outperforms the SDR-based method significantly. For instance, the extra gain needed for the SDR method is 4 dB compared with the proposed method for a desired $P_D = 0.95$.
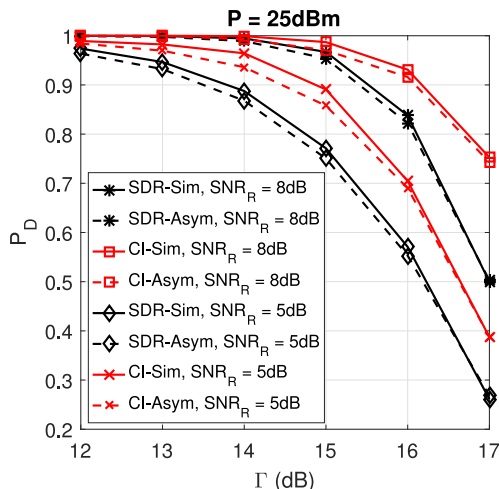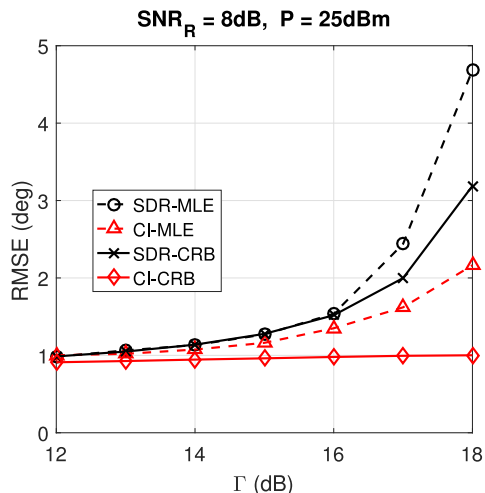

Fig. 9.　RMSE vs. SINR threshold for different power budget, $\text{SNR}_R = 8$ dB, $P = 25$ dBm, QPSK.

Fig. 8 shows another important trade-off between radar and communication, where the detection probability at the radar with increased SINR threshold of the downlink users are provided for the two methods with $P = 25$ dBm. It can be seen that a higher SINR requirement at users leads to a lower P_D for radar, and the proposed method obtains better trade-off curves for both simulated and asymptotic results thanks to the utilization of MUI. The results in Figs. 7 and 8 justify the use of the Gaussian radar detector of (44) for the CI beamformer, which still gives significant performance gains w.r.t the SDR beamformer.

In Fig. 9, the root mean squared error (RMSE) of the target DoA estimation with the presence of the minimized BS interference is given for CI and SDR beamformers, both with increased SINR threshold. Here the maximum likelihood estimator defined by (43) is used as the concrete DoA estimation algorithm, and the corresponding CRB curves are given by (53). As expected, the loose of the communication constraints in CI methods brings benefits to radar target estimation. It can be also
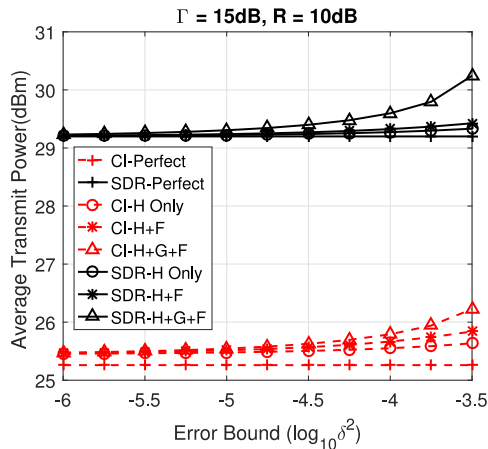
Fig. 10. Average transmit power vs. error bound for different robust cases, $\Gamma = 15\,\text{dB}, R = 10\,\text{dB}$, QPSK.
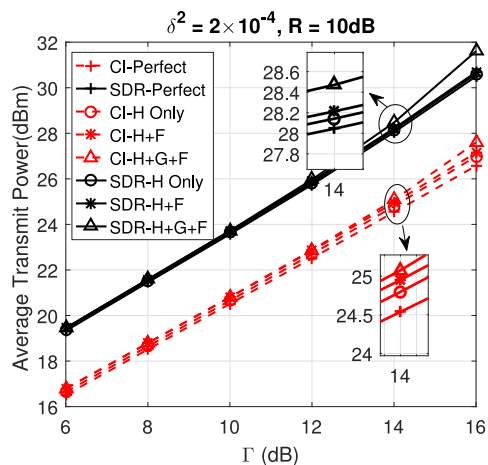

Fig. 11. Average transmit power vs. SINR for different robust cases, $\delta^2 = 2 \times 10^{-4}, R = 10\,\text{dB}$, QPSK.

observed that the proposed approach is not only robust to the increasing SINR requirement, but also performs far better than the SDR method.

D. Robust Designs

In Fig. 10, the BS transmit power with increasing CSI error bound δ is shown with $\Gamma = 15\,\text{dB}, R = 10\,\text{dB}$, where different cases with perfect and imperfect CSI are simulated for both SDR and CI-based beamforming. The legend denotes the channel which suffers from CSI errors for each case, while the rest are assumed perfectly known. Thanks to its relaxed nature, the CI-based beamforming has a higher degree of tolerance for the CSI errors than SDR-based ones. The same trend is also shown in Fig. 11, where we apply a fixed channel error bound $\delta^2 = 2 \times 10^{-4}$ and $R = 10\,\text{dB}$ for all the robust cases to see the variation of the transmit power with an increased SINR level. Since the interference channel between radar and users should first be estimated by the users and then fed back to the BS, the knowledge about $\mathbf{F}$ is more likely to be known inaccurately by the BS compared with other two channels. Fortunately, we

observe that in both Figs. 10 and 11, the imperfect channel $\mathbf{F}$ requires less transmit power to meet the same SINR level than $\mathbf{H}$ and $\mathbf{G}$ with CSI errors of the same bound. Hence, the accuracy for the estimation of $\mathbf{F}$ can be relatively lower than the other channels.

VIII. CONCLUSION

This paper proposes a novel optimization-based beamforming approach for MIMO radar and downlink MU-MISO communication coexistence, where multi-user interference is utilized to enhance the performance of communication system and relax the constraints in the optimization problems. Numerical results show that the proposed scheme outperforms the conventional SDR-based beamformers in terms of both power and interference minimization. An efficient gradient projection method is further given to solve the proposed power minimization problem, and is compared with SDR-based solver in the sense of average execution time. While the proposed technique is applied at symbol level, the computation complexity is still comparable with the SDR approach in typical LTE systems. Moreover, the detection probability and the Cramér-Rao bound for MIMO radar in the presence of the interference from BS are analytically derived, and the trade-off between the performance of radar and communication is revealed. Finally, a robust beamformer for power minimization is designed for imperfect CSI cases based on interference exploitation, and obtains significant performance gains compared with conventional schemes.

REFERENCES

[1] FCC, Connecting America: The National Broadband Plan, 2010. [Online]. Available: https://www.fcc.gov/general/national-broadband-plan

[2] J. R. Guerci, R. M. Guerci, A. Lackpour, and D. Moskowitz, "Joint design and operation of shared spectrum access for radar and communications," in *Proc. 2015 IEEE Radar Conf.*, May 2015, pp. 0761–0766.

[3] D. W. Bliss, "Cooperative radar and communications signaling: The estimation and information theory odd couple," in *Proc. 2014 IEEE Radar Conf.*, May 2014, pp. 0050–0055.

[4] A. R. Chiriyath, B. Paul, G. M. Jacyna, and D. W. Bliss, "Inner bounds on performance of radar and communications co-existence," *IEEE Trans. Signal Process.*, vol. 64, no. 2, pp. 464–474, Jan. 2016.

[5] S. D. Blunt, P. Yatham, and J. Stiles, "Intrapulse radar-embedded communications," *IEEE Trans. Aerosp. Electron. Syst.*, vol. 46, no. 3, pp. 1185–1200, Jul. 2010.

[6] S. D. Blunt, J. G. Metcalf, C. R. Biggs, and E. Perrins, "Performance characteristics and metrics for intra-pulse radar-embedded communication," *IEEE J. Sel. Areas Commun.*, vol. 29, no. 10, pp. 2057–2066, Dec. 2011.

[7] F. Liu, L. Zhou, C. Masouros, A. Li, W. Luo, and A. Petropulu, "Towards dual-functional radar-communication systems: Optimal waveform design," 2017. [Online]. Available: https://arxiv.org/abs/1711.05220

[8] F. Liu, C. Masouros, A. Li, H. Sun, and L. Hanzo, "MU-MIMO communications with MIMO radar: From co-existence to joint transmission," *IEEE Trans. Wireless Commun.*, vol. 17, no. 4, pp. 2755–2770, Apr. 2018.

[9] B. J. Donnet and I. D. Longstaff, "Combining MIMO radar with OFDM communications," in *Proc. 2006 Eur. Radar Conf.*, Sep. 2006, pp. 37–40.

[10] S. Sodagari, A. Khawar, T. C. Clancy, and R. McGwier, "A projection based approach for radar and telecommunication systems coexistence," in *Proc. 2012 IEEE Global Commun. Conf.*, Dec. 2012, pp. 5010–5014.

[11] A. Khawar, A. Abdelhadi, and C. Clancy, "Target detection performance of spectrum sharing MIMO radars," *IEEE Sens. J.*, vol. 15, no. 9, pp. 4928–4940, Sep. 2015.

[12] J. A. Mahal, A. Khawar, A. Abdelhadi, and T. C. Clancy, "Spectral coexistence of MIMO radar and MIMO cellular system," *IEEE Trans. Aerosp. Electron. Syst.*, vol. 53, no. 2, pp. 655–668, Apr. 2017.

[13] B. Li and A. Petropulu, "MIMO radar and communication spectrum sharing with clutter mitigation," in *Proc. 2016 IEEE Radar Conf.*, May 2016, pp. 1–6.

[14] B. Li, A. P. Petropulu, and W. Trappe, "Optimum co-design for spectrum sharing between matrix completion based MIMO radars and a MIMO communication system," *IEEE Trans. Signal Process.*, vol. 64, no. 17, pp. 4562–4575, Sep. 2016.

[15] A. Abdelhadi and T. C. Clancy, "Network MIMO with partial cooperation between radar and cellular systems," in *Proc. 2016 Int. Conf. Comput., Netw. Commun.*, Feb. 2016, pp. 1–5.

[16] K. T. Phan, S. A. Vorobyov, N. D. Sidiropoulos, and C. Tellambura, "Spectrum sharing in wireless networks via QoS-aware secondary multicast beamforming," *IEEE Trans. Signal Process.*, vol. 57, no. 6, pp. 2323–2335, Jun. 2009.

[17] H. Du and T. Ratnarajah, "Robust utility maximization and admission control for a MIMO cognitive radio network," *IEEE Trans. Veh. Technol.*, vol. 62, no. 4, pp. 1707–1718, May 2013.

[18] F. Liu, C. Masouros, A. Li, and T. Ratnarajah, "Robust MIMO beamforming for cellular and radar coexistence," *IEEE Wireless Commun. Lett.*, vol. 6, no. 3, pp. 374–377, Jun. 2017.

[19] Z. Q. Luo, W. K. Ma, A. M. C. So, Y. Ye, and S. Zhang, "Semidefinite relaxation of quadratic optimization problems," *IEEE Signal Process. Mag.*, vol. 27, no. 3, pp. 20–34, May 2010.

[20] A. B. Gershman, N. D. Sidiropoulos, S. Shahbazpanahi, M. Bengtsson, and B. Ottersten, "Convex optimization-based beamforming," *IEEE Signal Process. Mag.*, vol. 27, no. 3, pp. 62–75, May 2010.

[21] E. Alsusa and C. Masouros, "Adaptive code allocation for interference management on the downlink of DS-CDMA systems," *IEEE Trans. Wireless Commun.*, vol. 7, no. 7, pp. 2420–2424, Jul. 2008.

[22] C. Masouros and E. Alsusa, "Two-stage transmitter precoding based on data-driven code-hopping and partial zero forcing beamforming for MC-CDMA communications," *IEEE Trans. Wireless Commun.*, vol. 8, no. 7, pp. 3634–3645, Jul. 2009.

[23] C. Masouros and E. Alsusa, "Soft linear precoding for the downlink of DS/CDMA communication systems," *IEEE Trans. Veh. Technol.*, vol. 59, no. 1, pp. 203–215, Jan. 2010.

[24] C. Masouros, "Correlation rotation linear precoding for MIMO broadcast communications," *IEEE Trans. Signal Process.*, vol. 59, no. 1, pp. 252–262, Jan. 2011.

[25] C. Masouros, M. Sellathurai, and T. Ratnarajah, "Vector perturbation based on symbol scaling for limited feedback MISO downlinks," *IEEE Trans. Signal Process.*, vol. 62, no. 3, pp. 562–571, Feb. 2014.

[26] C. Masouros and G. Zheng, "Exploiting known interference as green signal power for downlink beamforming optimization," *IEEE Trans. Signal Process.*, vol. 63, no. 14, pp. 3628–3640, Jul. 2015.

[27] F. Liu, C. Masouros, P. V. Amadori, and H. Sun, "An efficient manifold algorithm for constructive interference based constant envelope precoding," *IEEE Signal Process. Lett.*, vol. 24, no. 10, pp. 1542–1546, Oct. 2017.

[28] P. V. Amadori and C. Masouros, "Large scale antenna selection and precoding for interference exploitation," *IEEE Trans. Commun.*, vol. 65, no. 10, pp. 4529–4542, Oct. 2017.

[29] A. Li and C. Masouros, "Exploiting constructive mutual coupling in P2P MIMO by analog-digital phase alignment," *IEEE Trans. Wireless Commun.*, vol. 16, no. 3, pp. 1948–1962, Mar. 2017.

[30] S. Timotheou, G. Zheng, C. Masouros, and I. Krikidis, "Exploiting constructive interference for simultaneous wireless information and power transfer in multiuser downlink systems," *IEEE J. Sel. Areas Commun.*, vol. 34, no. 5, pp. 1772–1784, May 2016.

[31] K. L. Law, C. Masouros, and M. Pesavento, "Transmit precoding for interference exploitation in the underlay cognitive radio Z-channel," *IEEE Trans. Signal Process.*, vol. 65, no. 14, pp. 3617–3631, Jul. 2017.

[32] P. V. Amadori and C. Masouros, "Constant envelope precoding by interference exploitation in phase shift keying-modulated multiuser transmission," *IEEE Trans. Wireless Commun.*, vol. 16, no. 1, pp. 538–550, Jan. 2017.

[33] P. V. Amadori and C. Masouros, "Interference-driven antenna selection for massive multiuser MIMO," *IEEE Trans. Veh. Technol.*, vol. 65, no. 8, pp. 5944–5958, Aug. 2016.

[34] I. Bekkerman and J. Tabrikian, "Target detection and localization using MIMO radars and sonars," *IEEE Trans. Signal Process.*, vol. 54, no. 10, pp. 3873–3883, Oct. 2006.

[35] M. Alodeh, S. Chatzinotas, and B. Ottersten, "Constructive interference through symbol level precoding for multi-level modulation," in *Proc. 2015 IEEE Global Commun. Conf.*, Dec. 2015, pp. 1–6.

[36] J. Li and P. Stoica, "MIMO radar with colocated antennas," *IEEE Signal Process. Mag.*, vol. 24, no. 5, pp. 106–114, Sep. 2007.

[37] B. Li and A. P. Petropulu, "Joint transmit designs for coexistence of MIMO wireless communications and sparse sensing radars in clutter," *IEEE Trans. Aerosp. Electron. Syst.*, vol. 53, no. 6, pp. 2846–2864, Dec. 2017.

[38] S. Boyd and L. Vandenberghe, *Convex Optimization*. Cambridge, U.K.: Cambridge Univ. Press, 2004.

[39] N. Meinshausen, "Sign-constrained least squares estimation for high-dimensional regression," *Electron. J. Statist.*, vol. 7, pp. 1607–1631, 2013. [Online]. Available: http://dx.doi.org/10.1214/13-EJS818

[40] S. Wright, *Numerical Optimization*. New York, NY, USA: Springer, 1999.

[41] A. Beck, "Convergence rate analysis of gradient based algorithms," Ph.D. dissertation, Tel-Aviv Univ., 2002.

[42] E. Karipidis, N. D. Sidiropoulos, and Z. Q. Luo, "Quality of service and max-min fair transmit beamforming to multiple cochannel multicast groups," *IEEE Trans. Signal Process.*, vol. 56, no. 3, pp. 1268–1279, Mar. 2008.

[43] Q. He, N. H. Lehmann, R. S. Blum, and A. M. Haimovich, "MIMO radar moving target detection in homogeneous clutter," *IEEE Trans. Aerosp. Electron. Syst.*, vol. 46, no. 3, pp. 1290–1301, Jul. 2010.

[44] S. M. Kay, *Fundamentals of Statistical Signal Processing: Detection Theory,* vol. 2. Englewood Cliffs, NJ, USA: Prentice Hall, 1998.

[45] S. M. Kay, *Fundamentals of Statistical Signal Processing: Estimation Theory,* vol. 1. Englewood Cliffs, NJ, USA: Prentice Hall, 1998.

[46] M. B. Shenouda and T. N. Davidson, "On the design of linear transceivers for multiuser systems with channel uncertainty," *IEEE J. Sel. Areas Commun.*, vol. 26, no. 6, pp. 1015–1024, Aug. 2008.

[47] H. Wang, J. T. Johnson, and C. J. Baker, "Spectrum sharing between communications and ATC radar systems," *IET Radar Sonar Nav.*, vol. 11, no. 6, pp. 994–1001, 2017.

[48] R. Saruthirathanaworakun, J. M. Peha, and L. M. Correia, "Opportunistic sharing between rotating radar and cellular," *IEEE J. Sel. Areas Commun.*, vol. 30, no. 10, pp. 1900–1910, Nov. 2012.

[49] M. Grant and S. Boyd, "CVX: MATLAB software for disciplined convex programming, Version 2.1," 2017. [Online]. Available: http://cvxr.com/cvx/

Fan Liu (S'16) received the Bachelor's degree in information engineering from the Beijing Institute of Technology, Beijing, China, in 2013, where he is currently working toward the Ph.D. degree in the School of Information and Electronics. From 2016 to 2018, he was with the Communications and Information Systems Research Group, Department of Electrical and Electronic Engineering, University College London, London, U.K., as a Visiting Student. His research interests include precoding designs for MIMO systems, signal detection and estimation, and convex optimization. He received the Marie Curie Individual Fellowship in 2018, and has been recognized as an Exemplary Reviewer for the IEEE TRANSACTIONS ON COMMUNICATIONS.

Christos Masouros (M'06–SM'14) received the Diploma degree in electrical and computer engineering from the University of Patras, Patras, Greece, in 2004, and the M.Sc. and Ph.D. degrees in electrical and electronics engineering from the University of Manchester, Manchester, U.K., in 2006 and 2009, respectively. In 2008, he was a Research Intern with the Philips Research Laboratories, U.K. From 2009 to 2010, he was a Research Associate with the University of Manchester, and from 2010 to 2012, a Research Fellow with Queen's University Belfast. He is currently an Associate Professor with the Communications and Information Systems Research Group, Department of Electrical and Electronic Engineering, University College London, London, U.K. His research interests include wireless communications and signal processing with particular focus on green communications, large-scale antenna systems, cognitive radio, interference mitigation techniques for MIMO, and multicarrier communications. He was the recipient of the Best Paper Award in IEEE GLOBECOM Conference 2015. From 2011 to 2016, he held the Royal Academy of Engineering Research Fellowship. He has been recognized as an Exemplary Editor for the IEEE COMMUNICATIONS LETTERS and an Exemplary Reviewer for the IEEE TRANSACTIONS ON COMMUNICATIONS. He is an Editor for the IEEE TRANSACTIONS ON COMMUNICATIONS, an Associate Editor for the IEEE COMMUNICATIONS LETTERS, and was a Guest Editor for the *IEEE Journal on Selected Topics in Signal Processing* issues "Exploiting Interference towards Energy Efficient and Secure Wireless Communications" and "Hybrid Analog/Digital Signal Processing for Hardware-Efficient Large Scale Antenna Arrays."

Ang Li (S'14) received the Ph.D. degree from the Communications and Information Systems Research Group, Department of Electrical and Electronic Engineering, University College London, London, U.K., in 2018. He is currently a Postdoctoral Research Associate with the School of Electrical and Information Engineering, University of Sydney, Sydney, Australia. His research interests include beamforming and signal processing techniques for MIMO systems.

Jianming Zhou received the Ph.D. degree from the School of Information and Electronics, Beijing Institute of Technology, Beijing, China, in 2004, where he is currently an Associate Professor. His research interests include radar-communication integration and ultrawideband radar systems.

Tharmalingam Ratnarajah (A'96–M'05–SM'05) is currently with the Institute for Digital Communications, University of Edinburgh, Edinburgh, U.K., as a Professor in digital communications and signal processing and the Head of the Institute for Digital Communications. His research interests include signal processing and information theoretic aspects of 5G and beyond wireless networks, full-duplex radio, mmWave communications, random matrices theory, interference alignment, statistical and array signal processing, and quantum information theory. He has published more than 330 publications in these areas and holds four U.S. patents.

He was the coordinator of the FP7 projects ADEL (3.7M) in the area of licensed shared access for 5G wireless networks, HARP (4.6M) in the area of highly distributed MIMO, FP7 Future and Emerging Technologies projects HIATUS (3.6M) in the area of interference alignment, and CROWN (3.4M) in the area of cognitive radio networks. He is a fellow of Higher Education Academy (FHEA), U.K.